Front. Environ. Sci. Eng. 2013, 7(3): 302–325
DOI 10.1007/s11783-013-0511-6

FEATURE ARTICLE

The abatement of major pollutants in air and water by environmental catalysis

Junhua LI (✉)[1], Hong HE[2], Chun HU[2], Jincai ZHAO (✉)[3]

1 Tsinghua University, State Key Joint Laboratory of Environment Simulation and Pollution Control, School of Environment, Beijing 100084, China
2 Chinese Academy of Science, Ecoenvironmental Science Research Center, Beijing 100085, China
3 Chinese Academy of Sciences, Institute of Chemistry, Beijing 100190, China

Abstract This review reports the research progress in the abatement of major pollutants in air and water by environmental catalysis. For air pollution control, the selective catalytic reduction of NO_x (SCR) by ammonia and hydrocarbons on metal oxide and zeolite catalysts are reviewed and discussed, as is the removal of Hg from flue gas by catalysis. The oxidation of Volatile organic compounds (VOCs) by photo- and thermal- catalysis for indoor air quality improvement is reviewed. For wastewater treatment, the catalytic elimination of inorganic and organic pollutants in wastewater is presented. In addition, the mechanism for the procedure of abatement of air and water pollutants by catalysis is discussed in this review. Finally, a research orientation on environment catalysis for the treatment of air pollutants and wastewater is proposed.

Keywords air pollution control, wastewater treatment, $DeNO_x$, selective catalytic reduction (SCR), Volatile organic compounds (VOCs), environmental catalysis

1 Introduction

Environmental protection is directly related to the sustainable development of economies and society. The control of the emission of major air and water pollutants remains a daunting challenge in China. The removal of major air pollutants (PM, SO_2, NO_x, Volatile organic compounds (VOCs) and Hg) from stationary and mobile sources is becoming increasingly urgent for the improvement of air quality, and the removal of thousands of industrial and natural chemical compounds from contaminated water systems is also critical to maintain the availability of clean water. Therefore, cost-effective and appropriate air-pollution-control and water-treatment technologies must be explored and implemented.

To date, some technological options exist to control air pollution and wastewater; however, the most efficient method is based on the principle of environmental catalysis. In this paper, the development of control technologies for environmental catalysis for air-pollution control and wastewater treatment is reviewed, and the abatement mechanism of air and water pollutants via catalysis is discussed.

Received November 3, 2012; accepted December 28, 2012

E-mail: lijunhua@tsinghua.edu.cn; jczhao@iccas.ac.cn,

2 Removal of NO_x and Hg in flue gas by catalysis

Air pollutants, such as NO_x and Hg, are mainly emitted from stationary sources, and the technology for control of their emissions can be grouped into source control and end control. The environmental catalysis method is the most efficient way to remove NO_x in end-control technology. For example, the SCR of NO_x with a reductant (typically NH_3) into water and nitrogen is an available method over a special catalyst, which is the key factor in achieving highly efficient NO_x conversion.

2.1 The development of NH_3-SCR catalysts

2.1.1 Chemical reaction and mechanism of NH_3-SCR at high temperature

The commercial catalysts for stationary sources, such as power plants and industrial boilers, are based on a high-temperature SCR (HT-SCR) catalyst, V_2O_5-WO_3 (or MoO_3)/TiO_2, that operates in the high-temperature range of 350°C–430°C [1]. V_2O_5 is the main active component for the catalytic reduction of NO_x, whereas WO_3 is used as an additive to increase the catalytic activity and the thermal

stability [2], and TiO_2 serves as a support. In past decades, numerous other formulations have been developed for the SCR reaction. Because vanadium species are poisonous to humans and to the environment, numerous researchers have contributed to the development of non-vanadium SCR catalysts.

At present, numerous transition metals have been reported to be active in NO_x reduction, including TiO_2-supported V_2O_5, Fe_2O_3, CuO, MnO_x and CeO_x catalysts [3–10]. Among metal oxides, pure V_2O_5 and V_2O_5 supported on oxide carriers (Al_2O_3, SiO_2, ZrO_2, TiO_2, etc.) have been extensively investigated. Metal oxides supported on active carbon have been proposed as a competitive choice compared with the available catalysts because of its economic efficiency. Studies have shown that metal oxides that are active as oxidation catalysis could mostly serve as an active component in the SCR reaction.

In most cases, NH_3 is used as the reductant in commercial SCR plants. In the presence of O_2, NH_3 reacts with NO_x to form water and nitrogen according to the general reactions:

$$4NO + 4NH_3 + O_2 \rightarrow 4N_2 + 6H_2O \quad (1)$$

$$2NO_2 + 4NH_3 + O_2 \rightarrow 3N_2 + 6H_2O \quad (2)$$

In practice, the following side reactions can also occur:

$$4NH_3 + 3O_2 \rightarrow 2N_2 + 6H_2O(> 350°C) \quad (3)$$

$$4NH_3 + 5O_2 \rightarrow 4NO + 6H_2O(> 350°C) \quad (4)$$

$$4NH_3 + 4O_2 \rightarrow 2N_2O + 6H_2O(> 350°C) \quad (5)$$

$$2NH_3 \rightarrow N_2 + 3H_2 \quad (6)$$

If SO_2 and H_2O are present in the combustion gases, the following reactions are possible over the catalyst:

$$SO_2 + 1/2\ O_2 \rightarrow SO_3 \quad (7)$$

$$NH_3 + SO_3 + H_2O \rightarrow NH_4HSO_4 \quad (8)$$

$$2NH_3 + SO_3 + H_2O \rightarrow (NH_4)_2SO_4 \quad (9)$$

$$SO_3 + H_2O \rightarrow H_2SO_4 \quad (10)$$

Even small amounts of SO_2 and H_2O are highly undesirable because they cause the deposition and accumulation of ammonium sulfate salts on the catalyst (if the temperature of the catalyst is not sufficiently high) and on the air-pre-heater downstream from the catalytic reactor.

Acidity and redox properties are both considered to be important parameters for SCR catalysts. Topsøe et al. [11] proposed the mechanistic scheme shown in Fig. 1. In this mechanism, the catalytic performance is related to the NH_3 adsorbed on the Brønsted acid sites associated with V^{5+}-OH sites. The catalytic cycle consists of both acid–base and redox reactions.

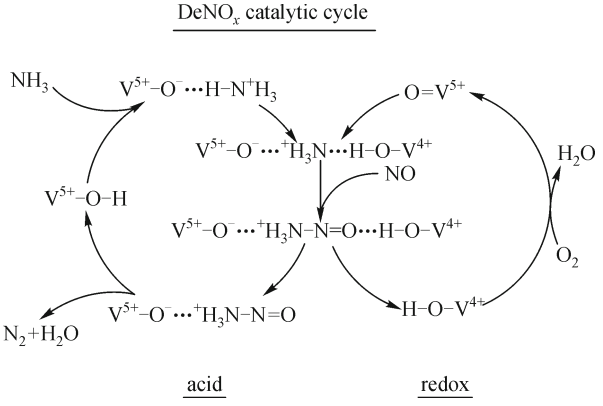

Fig. 1 Mechanistic scheme of the catalytic cycle of the SCR reaction over the V_2O_5/TiO_2 catalyst in the presence of oxygen [11]

2.1.2 Recent developments in LT-SCR catalysts

Although SCR technology based on vanadia catalysts has been introduced into the market for the removal of NO_x from flue gas, some problems still remain due to the toxicity of active vanadium, the significant amount of N_2O formed at high temperatures, and the high activity toward the oxidation of SO_2 to SO_3 [12]. Low-temperature SCR (LT-SCR) catalysts, which can work well at approximately 250°C or at even lower temperatures and allow the SCR unit be placed behind the desulfurizer in a power plant, have attracted much attention in the academic and industrial field. Hence, many researchers continue to develop new LT-SCR catalysts. The development of this type of catalyst has been well summarized in a recent review [13]. Some vanadium free transition-metal-based oxide catalysts, such as $FeTiO_x$ [14], CuO_x/WO_x-ZrO_2 [15], WO_3/CeO_2-ZrO_2 [16] and Ce/TiO_2 [17,18], have also been reported as potential substitutes of vanadium-based catalysts. Recently, Ce-W-Ti and Ce-W mixed oxide catalysts, which showed excellent NH_3-SCR activity and high N_2 selectivity over a wide range of operating temperatures and extremely high resistance to space velocity have been reported [19,20].

The development of LT-SCR catalysts for the removal of NO_x by NH_3 is still a substantial challenge, especially at temperatures less than 200°C. According to the literature, many catalysts that contain transition metals (such as Fe, V, Cu or Mn) exhibit low-temperature SCR activity, among which, the MnO_x catalyst has demonstrated excellent low-temperature performance and has been researched extensively [21].

Kijlstra [22] has reported that the conversion rate of NO_x is 72% over a MnO_x/Al_2O_3 catalyst at 150°C; however, the catalyst is not stable. In the first 50 h, the conversion rate decreases rapidly and later gradually becomes steady at approximately 40%. The preparation method affects the activity of Mn-based catalysts. Tang et al. [23] investigated manganese oxide catalysts prepared using different methods and found that the crystallinity of MnO_x was affected by the preparation method. MnO_x with lower crystallinity, such as MnO_x (SP, solid-phase reaction method) and MnO_x (CP, co-precipitation method), exhibited higher activity at low temperatures. The specific surface area and oxidation state of the Mn in MnO_x are both correlated to the SCR activity to some extent [24].

The MnO_x-CeO_2 catalyst has been investigated extensively because of its superior performance [25,26]. Qi et al. [25] found that the Mn/(Mn + Ce) molar ratio and calcination temperature influence the activity significantly. The results suggested that the reaction was zero order with respect to NH_3 and first order with respect to NO over this catalyst. The addition of Fe, Zr [27] or Nb [28] would improve the low-temperature activity and N_2 selectivity.

Various support materials have been employed in LT-SCR catalysis. They can be divided into metal oxides, carbon materials and zeolites. The dispersion of active sites depends on the concentration of the precursor solution, the method by which the metal is introduced, and the final procedure of drying [29]. All of these factors correlate to the structure and performance of the catalyst. The development of this type of catalyst has been well summarized in a recent review [24].

With respect to the LT-SCR reaction, many researchers have proposed that NH_3 is adsorbed onto a Lewis acid center and that intermediates such as NH_2 [27,30] and adsorbed NH_3 [31] are formed. The intermediates react with aerial NO_2 through the Eley–Rideal (E–R) mechanism or with nitrite species through the Langmuir–Hinshelwood (L–H) mechanism [32]. The SCR mechanism at different temperature was shown in Fig. 2. The presence of O_2 is necessary for the formation of NH_2 and activated NO_2 intermediates.

2.2 Factors that affect the NH_3-SCR reaction

2.2.1 Effects of H_2O and SO_2

The effects of water vapor can be divided into reversible and irreversible effects. Co-adsorption with NH_3 or NO on the active sites is considered to be an important factor with respect to H_2O, which influences the catalytic activity and the light-off temperature. For the SCR of NO_x by NH_3 in the absence of SO_2, the effect of H_2O is not severe at high temperatures. However, the more direct participation of water in the mechanism of the $DeNO_x$ reaction should be studied in the future.

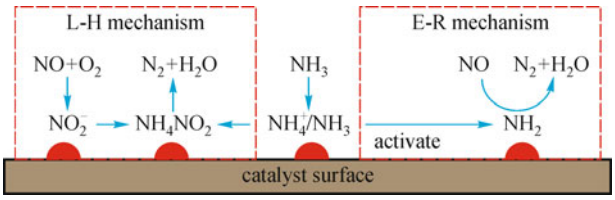

Fig. 2 Mechanism of NH_3-SCR of NO over Mn-Fe catalysts [32]

When H_2O and SO_2 coexist, SO_2 can be oxidized to SO_3 and further oxidized to H_2SO_4 and sulfates with SCR catalysts. The effect of SO_2 originates from two aspects: 1) corrosion of pipes and plants downstream by SO_3, which is generated from SO_2 oxidation; 2) covering of the active sites by metal sulfates and ammonium sulfates [22]. This second effect is regarded as the main reason for the decrease in SCR activity. The TOF of SO_2 oxidation (SO_2 molecules converted per surface redox site per second) of TiO_2-supported catalysts were all within an order of magnitude ($V_2O_5/TiO_2 > Fe_2O_3/TiO_2 > Re_2O_7/TiO_2 \sim CrO_3/TiO_2 \sim Nb_2O_5/TiO_2 > MoO_3/TiO_2 \sim WO_3/TiO_2$). The mechanism of SO_2 oxidation is not sensitive to the synergy of the surface metal oxide species [33]. The content of V_2O_5 is usually kept low (less than 2 wt. %) because it is active not only in the SCR reaction but also in the oxidation of SO_2 [34].

Sulfate species, which can be produced from SO_2 oxidation, played dual roles with respect to catalytic activity, which depends on temperature. At temperatures greater than 300°C, catalytic activity is generally enhanced because of the enhanced intensity of Brønsted acid sites by the adsorbed sulfate species. At temperatures less than 200°C, the formation of metal sulfates leads to a disruption of the redox properties between active sites [35]. The accumulation of sulfate species on the catalyst surface will lead to the irreversible destruction of the surface catalytic centers involved in the oxidation of NO to NO_2 [36]. The catalytic activity decreased rapidly in the presence of SO_2. In the temperature range of 200°C–300°C, both roles of sulfate exist, and the effect of sulfation depends on the catalyst morphology and the mechanism of SCR reaction.

Numerous components, such as Cu and Fe, were found to be effective to improve the SO_2 resistance of SCR catalysts compared to that of the Mn-based catalyst [37–39]. The addition of an additive, such as by the doping of SnO_2 [26,40], is another way to possibly solve this problem, and this approach resulted in an enhanced activity at low temperature and increased N_2 selectivity.

2.2.2 Effect of alkali and alkaline-earth metals

Alkali or alkaline-earth metal oxides and/or salts (alkali) that originate from the flow gas of bio-fuel plants [41,42], municipal solid-waste incineration plants [43], diesel-fuel engines [44,45], and coal-fired plants are a serious threat

and a major concern to the industrial utilization of SCR catalysts. The deposition of these species can significantly reduce the SCR performance and limit the catalyst's lifetime.

The effect of alkali metals on traditional V_2O_5-WO_3/TiO_2 catalysts has been widely studied, and the deactivation is attributed to the decreased acidity of the catalysts [46]. Kamata et al. [47] have studied the effect of K_2O on the traditional catalyst and proposed that the potassium oxide partially reacted with V_2O_5 to form KVO_3. Khodayari et al. [41,48] reported that potassium retarded the redox potential of the surface vanadia species and decreased the amount of NH_3 adsorbed: the amount of NH_3 (ad) bound to the Brønsted-acid sites decreased with increasing potassium content of the catalyst, whereas the amount of NH_3 (ad) adsorbed onto the Lewis-acid sites was nearly unchanged. Lisi et al. [43] proposed that K and Na did not cause a loss of surface area but rather caused a significant decrease in the surface acidity. Zheng et al. [42] studied the deactivation effect of potassium in the form of both chloride and sulfate on the SCR catalysts and found that potassium titrated the active sites for NH_3 adsorption and that simply increasing the reaction temperature or the vanadium content cannot effectively compensate the loss of activity. Catalysts with high vanadium content become active for the oxidation of NH_3, which causes a net NO formation. Kröcher and coworkers [44] reported that the poisoning elements potassium and calcium occupied the non-atomic hole sites of the (010) V_2O_5 surface such that both Brønsted acid and V^{5+}-O sites were blocked. Klimczak et al. [45] proposed that, in addition to the deactivation by potassium, sodium, manganese and calcium, phosphate is also a strong deactivating component. Though doping of phosphorus on the catalyst surface could increase the acidity of the catalyst, the formation of phosphate results in a decreased catalytic surface due to pore blocking. All these studies have primarily focused on the effects of the surface acidity with decreasing SCR activity, and few reports have been devoted to the effects on other properties. Tang et al. [49] reported that the redox property (reducibility) could be another key factor for the poisoning effect of alkali metals over V_2O_5/TiO_2 based on the doping of sodium and calcium ions. Chen et al. [50] proposed that surface-chemisorbed oxygen could also be reduced and that the downward trend was in good agreement with the SCR activity. With respect to theoretical calculations, Calatayud et al. [51] investigated the stability and reactivity of the V_2O_5 (110) and (001) surfaces using the density functional theory (DFT) method. Moreover, they studied the effect of alkali doping on the V_2O_5/TiO_2 catalyst model and concluded that the dopant atoms significantly affect the V = O groups. Recently, Peng and Li et al. employed a combination of experimental and theoretical methods to elucidate the mechanism of the alkali metal deactivation of the CeW catalyst in SCR reactions [52]. They found that the decreases in the reducibility and the quantity of Brønsted acid sites were responsible for the catalyst deactivation and that the acid strength was not significantly influenced by the alkali metal. DFT calculations revealed that Na and K could easily adsorb onto the CeW (110) surface and that the surface oxygen could migrate to cover the active tungsten. More importantly, the CeW catalyst exhibited better resistance to alkali metal poisoning compared with that of the traditional V_2O_5/TiO_2 catalyst, and hot-water washing was found to be a convenient and effective method to regenerate alkali metal poisoned CeW catalysts.

2.3 Elemental mercury oxidization by catalysis

Mercury is an important air pollutant because of its toxic effects on the environment and human health, its persistence in the environment, and its global transport in air masses. Coal-fired utility boilers are currently the largest single known source of anthropogenic mercury emissions. The emission of mercury from coal-fired plants is a serious concern in both developed and developing countries [53]. Elemental mercury is the major species emitted in the flue gas from coal-fired utilities [54]. Thus far, the most promising and cost-effective technology for the control of elemental mercury emissions is the co-benefit of the SCR unit [55]. Gaseous elemental mercury can be catalytically oxidized to gaseous $HgCl_2$ via a SCR catalyst using HCl in the flue gas as the oxidant. The formed $HgCl_2$ can then be efficiently captured by wet flue-gas desulfurization (FGD) systems [56].

Laboratory, pilot and field tests verify that a commercial SCR catalyst (V_2O_5-WO_3/TiO_2) can oxidize elemental mercury to $HgCl_2$ in the presence of HCl [57,58]. However, without HCl, the ability of a commercial SCR catalyst for the transformation of elemental mercury is very poor. Ammonia, which is necessary for NO_x control, is a severe interferent for elemental mercury oxidization [59]. Alkali and alkaline-earth metals (Na, K, Mg and Ca) show an obvious deactivation for the oxidation of gaseous elemental mercury on a V_2O_5-WO_3/TiO_2 catalyst [60]. Furthermore, some other SCR catalysts, such as V_2O_5/TiO_2 [57], CeO_2/TiO_2 [35,61], Fe-Ti spinel [62], Fe-Ti-V spinel [63] and CeO_2-WO_3/TiO_2 [64,65], have shown excellent ability to oxidize elemental mercury. Recently, the commercial SCR catalyst has been modified by RuO_2 to suppress the interference of NH_3. Although a RuO_2-modified commercial SCR catalyst shows better efficiency for elemental mercury oxidization and excellent anti-deactivation ability for NH_3, its SCR activity obviously decreases at high temperatures because of the over-oxidization of NH_3.

Low-temperature SCR catalysts are extremely restricted in their application due to the deposition of ammonium bisulfate [66]. The installation of the SCR catalyst downstream from the particulate control device specifically for the purpose of elemental mercury oxidation may

be an economical choice because better mercury conversion can be achieved [55]. Therefore, numerous low-temperature SCR catalysts, such as MnO_x/TiO_2 [67], Mn-Fe spinel [62], Fe-Ti-Mn spinel [32] and MnO_x/Al_2O_3 [68], have been investigated for elemental mercury oxidization. The chemical adsorption of elemental mercury and elemental mercury oxidization is difficult to discriminate on low-temperature SCR catalysts.

The L–H mechanism, the E–R mechanism, and the Mars–Maessen mechanism have been employed to describe the reaction mechanism of the heterogeneous oxidization of elemental mercury on SCR catalysts (shown in Fig. 2). Elemental mercury first adsorbs onto the SCR catalyst, and the adsorbed elemental mercury subsequently reacts with gaseous HCl to form gaseous $HgCl_2$, which is the E–R mechanism [69]. In the L–H mechanism, both gaseous elemental mercury and HCl adsorb onto the SCR catalyst, and then the adsorbed elemental mercury reacts with adsorbed HCl to form $HgCl_2$ [70]. On some SCR catalysts, gaseous elemental mercury may compete with gaseous HCl for the adsorption sites. In the Mars–Maessen mechanism, elemental mercury first adsorbs onto the SCR catalyst, and the adsorbed elemental mercury is then oxidized by the lattice oxygen on the SCR catalyst to form HgO/Hg_2O, and the HgO/Hg_2O can react with gaseous HCl or adsorbed HCl to form $HgCl_2$ [71].

To date, none of these mechanisms has been verified as the dominant mechanism for catalytic mercury oxidation. If the SCR catalyst undergoes changes or if the reaction temperature varies, the mechanism for elemental mercury oxidization may be different. Furthermore, these mechanisms have been used to interpret the interference of SO_2 and NH_3 with elemental mercury oxidization over the SCR catalyst. Gaseous NH_3 may compete with elemental mercury for the adsorption sites, which would result in an obvious interference with elemental mercury oxidization [56]. SO_2 can react with the SCR catalyst and result in the sulfation of the SCR catalyst. The adsorption of elemental mercury and/or HCl onto the SCR catalyst may be restrained due to the sulfation. Furthermore, gaseous SO_2 may compete with elemental mercury and/or HCl for the adsorption sites [72]. As a result, SO_2 generally shows a remarkable interference with elemental mercury oxidization.

3 Removal of NO_x from automobile exhaust by catalysis

Among the new emerging SCR systems for automotive NO_x control, many efforts have been focused on metal-promoted zeolites. Many ion-exchange zeolites have been reported to be active in the NH_3-SCR reaction. Among this wide family of catalysts, iron and copper zeolites appear to be particularly interesting and have been extensively studied.

3.1 NH_3-SCR on zeolite catalysts

Metal-exchanged zeolites have been proven to be active SCR catalysts with broad operation-temperature windows [73]. Among these catalysts, Cu- and Fe-based zeolites are the most attractive catalysts for NH_3-SCR and have been extensively studied [73,74]. Cu-ZSM-5 and Cu-BETA are known to exhibit excellent low-temperature activity in this reaction. Isolated Cu^{2+} and Cu-O-Cu dimeric species are generally recognized to play key roles in the NH_3-SCR reaction, and the redox cycle between Cu^{2+} and Cu^+ is important [75,76]. However, Cu-ZSM-5 and Cu-BETA demonstrate a lack of hydrothermal stability at temperatures greater than 700°C. The change of oxidation state of copper during aging (the decrease of the Cu^+ species and/or agglomeration of Cu species) and the destruction of zeolite structure have been suggested to be the main reasons for hydrothermal deactivation. Fe-exchanged zeolites, especially Fe-ZSM-5, have been proven to be active catalysts for the NH_3-SCR of NO_x [73,77]. The NH_3-SCR activity of Fe-ZSM-5 can be affected by numerous parameters, including the Si/Al ratio of the zeolite, the degree of ion exchange and the preparation method [77–80]. The Fe species on Fe-ZSM-5 are generally distinguished as isolated Fe^{3+}, oligomeric Fe_xO_y clusters and Fe_2O_3 particles [77–80]. The contribution of different Fe species on Fe-ZSM-5 to SCR activity has been suggested to strongly depend on reaction temperature; however, isolated Fe^{3+} species should be the active sites for low-temperature SCR reactions. The limited hydrothermal stability of Fe-ZSM-5 catalysts is also one of the challenges for practical applications [81,82]. Hydrothermal aging is known to lead to the dealumination of zeolite frameworks, the migration of Fe ions to form Fe_xO_y clusters and a decrease of Brønsted acidity.

Recently, Cu-chabazite SCR catalysts (Cu-CHA), including Cu-SSZ-13 and Cu-SAPO-34 with high deNO_x efficiency, have been reported [83,84]. The CHA zeolite contains small-sized pores, which can coordinate isolated mononuclear Cu^{2+} species, and the CHA zeolite has shown excellent low-temperature NH_3-SCR activity and high resistance to hydrothermal aging and hydrocarbon poisoning. Further research has demonstrated that Cu-CHA catalysts can withstand severe hydrothermal aging conditions at 800°C for 16 h, which compares well with a vehicle-aged catalyst used for a 135,000 miles [85]. Attractively, the Cu-SSZ-13 catalyst still exhibited excellent N_2 selectivity with little N_2O produced, even though a significant amount of NO_2 existed in the feed gas [86]. All of these advantages indicate that the Cu-CHA is a promising catalyst for the DeNO_x process from diesel exhaust. More recently, a one-pot synthesis method with a significantly lower cost was designed for the preparation of Cu-SSZ-13 catalyst, which would be beneficial to the industrial application of Cu-SSZ-13 catalyst [87].

With respect to Fe-zeolite catalysts, research results have

shown that low iron loadings and low calcination temperatures resulted in mostly iron monomers, especially for the ion-exchanged samples [80,89]. In contrast, a mixture of monomers, oligomers and hematite particles was formed at intermediate to high loadings. Heating in this gas mixture gave a distinct correlation between the catalytic performance and the oxidation state of iron, which is more pronounced in the catalysts where mostly iron monomers are present. The Fe/HBEA catalysts have been recently developed for the NH_3-SCR reaction. Its possible mechanism in the so-called standard SCR reaction was elucidated by Klukowski, which is shown in Fig. 3 [90]. Their results suggested a dual-site mechanism, which implies that the NO and NH_3 adsorb and react on neighboring Fe^{3+} sites and that NH_3 undergoes several adsorption/desorption cycles on the substrate before adsorbing and reacting on the Fe^{3+} sites. The uptake of NH_3 results in the partial reduction of Fe^{3+} sites, which are finally recycled by O_2. However, some contribution from a single-site mechanism cannot be completely ruled out. SCR reaction mechanisms over zeolites at low temperatures have been summarized elsewhere [13].

3.2 HC-SCR technique

Among the NO_x reduction technologies developed for the control of diesel engine emissions, the selective catalytic reduction by hydrocarbon (HC-SCR) approach has attracted attention as a possible alternative to the NH_3 urea-SCR reaction [91,92]. The distinct advantage of HC-SCR is that the on-board fuel can be used as a reductant for NO_x conversion, which reduces the cost involved in the development of infrastructure for delivering reductant to an automotive engine exhaust system. Numerous catalysts, such as zeolite oxides, basic oxide/metal and noble-metal catalysts have been found to be effective for the HC-SCR of NO_x by CH_4, C_2H_2, C_2H_5OH in the presence of excess oxygen [92–97]. Among them, Ag/Al_2O_3 is known as one of the most effective catalysts for HC-SCR [98–100]. When using oxygenated hydrocarbons as reductants, particularly ethanol, Ag/Al_2O_3 shows high activity even in the presence of SO_2 and H_2O [101].

To improve the overall performance of Ag/Al_2O_3 for NO_x reduction, numerous researchers have focused on the relationship between the structural features of Ag/Al_2O_3 catalysts and their catalytic activity for the SCR of NO_x. NO_x reduction is widely accepted as being strongly correlated to the silver loading. Structural characterization, particularly by ultraviolet–visible spectroscopy (UV–vis), X-ray adsorption spectroscopy (XAS), and X-ray photoelectron spectroscopy (XPS) measurements, identified that oxidized silver was predominant on Ag/Al_2O_3 catalysts with moderate silver loadings, whereas metallic silver clusters (Ag_n^0) became dominant on high-silver-content alumina catalysts [100,102–107]. In general, oxidized silver present as isolated Ag^+ cations and/or oxidized silver clusters ($Ag_n^{\delta+}$) on the Al_2O_3 surface are responsible for the HC-SCR reaction, whereas metallic silver clusters are responsible for the direct combustion of hydrocarbons.

The structure of hydrocarbons is widely accepted as strongly influencing the activity of Ag/Al_2O_3 for NO_x reduction [91,92]. The oxygenated hydrocarbons, such as ethanol, acetaldehyde, and propyl alcohol, exhibit excellent NO_x reduction activity on Ag/Al_2O_3. Thus, elucidation of the intrinsic property responsible for the NO_x reduction by oxygenated hydrocarbons may provide a guideline for the development of a HC-SCR system with high efficiency for NO_x reduction. During the partial oxidation of ethanol and the reduction of NO_x with ethanol over Ag/Al_2O_3, large amounts of surface enolic species were observed by He and coworkers [92,108,109]. The surface enolic species exhibited much higher activity than did acetate in reactions with nitrate and/or NO + O_2 to form-NCO species, which demonstrates its crucial role in the SCR of NO_x by ethanol. Further studies have determined that enolic species also play a key role in the reduction of NO_x by other alcohols (1-propanol, isopropyl alcohol, 1-butanol, *sec*-butyl alcohol, and isobutyl alcohol) over Ag/Al_2O_3 [110–113], acetaldehyde over both Ag/Al_2O_3 [108] and Co/Al_2O_3 [114], and acetylene over ZSM-5 [115]. Interestingly, enols have been demonstrated to be the common intermediates in hydrocarbon oxidation [116]. More recently, Yan et al. [117] found that the enolic species that originate from the partial oxidation of ethanol over Ag/Al_2O_3 prefer to adsorb onto or close to silver sites, in intimate contact with the active phase. This adsorption behavior of this enolic species contributes to its high activity for the formation of isocyanate species (-NCO) and the final product, N_2, during the NO_x reduction by ethanol over Ag/Al_2O_3. These results strongly suggest that adsorbed enolic species and/or enols in the gas phase are the important intermediates involved in the HC-SCR of NO_x.

3.3 NSR technique

For decades, researchers have been committed to the

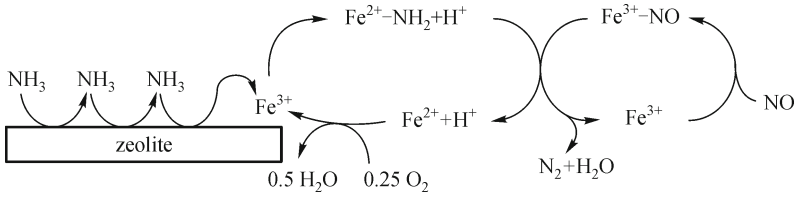

Fig. 3 Scheme of the proposed mechanism of the standard SCR reaction on Fe/HBEA zeolite [90]

development of new technologies to eliminate NO_x emissions from lean-burn exhaust. One of the promising solutions is the use of NO_x storage reduction (NSR, also known as lean NO_x trap (LNT) catalysts) [118]. The NSR catalyst, which was first developed by the Toyota Company, usually contains noble metals (Pt, Pd or Rh), alkali or alkaline-earth metals (e.g., Ba), and a high-surface-area support. This catalyst is supposed to reduce NO_x emissions under a cyclic lean/rich mode for diesel or lean-burn gasoline engines. In the operation of a typical lean engine, NO is oxidized to NO_2 over noble metals and is then stored as nitrites and/or nitrates on the storage components of the catalysts [119,120]. After the engine is periodically switched to fuel-rich conditions, the absorbed NO_x is released and reduced to N_2 by hydrogen, carbon monoxide, and hydrocarbons.

Most previous studies have focused on catalyst compositions that strongly affect the storage and reduction of NO_x [121]. Commonly, Al_2O_3 has been used as the support for NSR catalysts because of its high surface area. Recent studies have reported that CeO_2 exhibits certain advantages, particularly in relation to its good oxygen storage capacity and its ability to maintain a high dispersion of noble metals and improve the water–gas shift reaction [122]. With respect to Ba-containing catalysts, the noble-metal species and their dispersion have been reported to lead to different NO oxidation activity in the lean phase [119], which directly influences subsequent adsorption onto Ba sites. Furthermore, Ba sites located in proximity to Pt are generally accepted as playing an important role during the trapping process. A spill-over mechanism has been proposed to explain such promising effects, which indicates that both oxygen and NO/NO_2 could easily migrate from Pt sites to nearby Ba sites and thus improve the adsorption efficiency [123]. Recently, a $Pt/Co/Ba/Al_2O_3$ catalyst was developed by Wang et al. [124], on which an intimate contact of Co with Ba/Al provides more active sites for NO adsorption, oxidation and desorption. As a result, the Pt and Co co-supported catalysts show better NO_x storage and reduction performance and higher N_2 selectivity compared to the traditional Pt-supported Ba/Al_2O_3 catalyst.

4 Removal of VOCs by catalysis

4.1 Catalytic oxidation of VOCs from industry

VOCs are major contributors to air pollution because of their toxicity to human health and their involvement in the formation of photochemical smog. VOCs pollution derives mainly from emissions of industrial processes and automobile exhausts [125]. With increasingly stringent environmental regulation, the development of effective methods to control VOCs emissions is urgently needed. Numerous different methods are available to control VOCs emissions, and each method has practical limitations for different organic compounds, concentrations, and emission sources [126]. One of the most effective and economically feasible VOCs removal technologies is the catalytic oxidation method [127] because catalytic oxidation can operate with dilute VOCs effluent streams ($< 1\%$ VOCs) and at much lower temperatures than conventional thermal incineration; the catalytic oxidation method therefore does not produce undesirable by-products, such as dioxins and NO_x. In addition, catalytic oxidation targets the destruction of pollutant compounds rather than transferring the pollutant to another phase, which is the case for condensation and adsorption technologies and is a drawback unless the recycling of VOCs present in high concentrations is a consideration.

The development of noble-metal catalysts and transition-metal oxides for the catalytic oxidation of VOCs has been widely explored for both halogenated and non-halogenated compounds [128,129]. The noble-metal-based catalysts, despite their higher costs, are preferred because of their high specific activity, their resistance to deactivation and their ability to be regenerated [130]. The catalytic performance of supported noble metals strongly depends on the preparation method, the type of precursor, he metal loading and particle size, and the nature of the support [131,132]. Moreover, the operating conditions used, such as concentrations of VOCs and oxygen, the overall gas flow rate, and the type of reactor (fixed-bed catalytic reactor or flow-through membrane reactor) also strongly influence the catalytic performance [133,134]. Pt- and Pd-based catalysts exhibit low light-off temperatures in the oxidation of hydrocarbons and other organic chemicals [130,135] and therefore are used extensively as active components in industrial catalytic formulations for the conversion of VOCs emitted from stationary and vehicle sources [136,137]. The activity of Pd is generally better than that of Pt in the conversion of methane; however, its activity is lower in the transformation of other organic compounds [138]. The resistance of Pd to thermal and hydrothermal sintering is also better than that of Pt; however, its behavior in the presence of poisons, such as sulfur-containing pollutants, is worse [130]. The catalytic activity of Pd-based catalysts is closely related to the state of the Pd species, their particle size, and their morphology [139]; therefore, the catalytic behaviors of Pd catalysts have been widely investigated. Pd species on catalyst surfaces are widely accepted as being divisible into three groups: the metallic (Pd^0) state, the oxidized state (PdO) and a mixture of both states (Pd^0/PdO), depending on the catalytic process [140]. Disagreement still remains as to which Pd state is active for the catalytic oxidation of VOCs; related factors include the structures of the VOCs, the reaction temperature and the nature of the catalyst carrier [141,142].

The industrial application of Pt- and Pd-based catalysts for VOCs control is still limited by cost and sensitivity to

poisoning by chlorine/chloride products during the oxidation of chlorinated VOCs [127,143]. Thus, non-noble-metal oxide catalysts have been developed as low-cost alternatives to the Pt- and Pd-based catalysts. Substantial effort has been made to improve the oxidation activity and resistance to poisoning of metal oxide catalysts, including $CoCrO_x$ [144,145], $MnCoO_x$ [146], $InSnO_x$ [147], $MnCeO_x$ [148–150], $MnCuO_x$ [151], $NiCoO_x$ mixed oxides [152], Ce-doped ZrO_2 [153], Mn-doped ZrO_2 [154] and MnO_x/TiO_2-CNTs [155]. In recent years, the influence of the structure of metal oxide catalysts on activity has been reported, and catalysts prepared with ordered meso-structures exhibited better activity than bulk catalysts with non-meso-structures [156,157]. Different preparation methods for mixed-metal oxides have also been investigated in the oxidation of VOCs, and these studies have reported the influence of the preparation methods on the activity [149,150,158].

Although several effective metal oxide catalysts have been developed for the combustion of VOCs, some challenges still remain. For example, ordered meso-porous chromium trioxide is very active for toluene oxidation [159], but the high toxicity of chromium causes serious catalyst disposal problems. The supported vanadia catalysts show excellent activity and stability for the simultaneous removal of VOCs and NO_x in the Cl_2–HCl environment [160]; however, the corrosive properties of vanadia catalysts inhibit their widespread application, particularly for wet flue gas streams. Therefore, further research is needed to develop novel environmentally friendly and highly effective metal oxide catalysts to not only improve removal efficiencies but also reduce costs for the treatment of a wide variety of VOCs from industrial sources. In addition, more fundamental research to understand the catalytic mechanisms involved in oxidation reactions is also crucial to the objective of developing appropriate industrial materials for the removal of VOCs.

4.2 Catalytic purification indoor air pollutants

An individual on average spends more than 90% of the day inside buildings and vehicles; therefore, indoor air quality has great effects on human health [125,161]. With the increasing public health concerns about hazardous indoor pollutants, how to eliminate indoor air pollutants such as formaldehyde (HCHO), BTX or microbes etc., has been recently received great attention from the scientific community [162]. Physical adsorption, photocatalysis and thermal catalysis are the most common methods for indoor air purification and therefore have been extensively studied.

4.2.1 Photocatalysis

Photocatalysis presents an alternative to physical adsorption methods in indoor air pollution abatement [162]. The common photocatalysts are primarily metal oxides or sulphides, i.e., TiO_2, ZnO, ZrO_2, SnO_2, WO_3, CeO_2, Fe_2O_3, Al_2O_3, ZnS and CdS [163]. Because of its superior photocatalytic activity, chemical stability, low cost and nontoxicity, TiO_2 has been extensively studied as a photocatalyst [164–166]. Under UV illumination, an electron is excited from the valence band to the conduction band of TiO_2, generating a positive hole in the valence band. Positive holes can oxidize OH^- or water on the surface of TiO_2 to produce hydroxyl radicals, and then the hydroxyl radicals can subsequently oxidize gaseous pollutants [163]. The organic and inorganic pollutants in the indoor air such as formaldehyde, acetaldehyde, benzene, toluene, acetone, ammonia and NO_x can all be photo-oxidized into CO_2, H_2O and mineral acids on TiO_2 or other photocatalysts [162,167–170]. Bacteria in the indoor air can also be removed by photocatalytic decomposition [171], which is also important for indoor air purification [172]. Because TiO_2 is only active upon UV excitation, there has been much effort to develop second-generation TiO_2 photocatalysts that can be operated not only under UV but also visible light irradiation [173,174]. Various techniques have been employed to enable it to operate under visible light irradiation. These techniques include surface modification via organic materials and semiconductor coupling, band gap modification by creating oxygen vacancies, and by doping with nonmetals or co-doping with nonmetals and metals [175]. VOCs and bacteria can be photodegraded under visible light irradiation on Fe-TiO_2 [176], N-TiO_2 [177], C-TiO_2 [178,179], Cu_xO/TiO_2 [180], TiO_2 hybridized with graphite-like carbon [181] and so on. Air-cleaning devices based on photocatalysts require an additional light source. Besides use in air-cleaning devices, indoor wall paint with second-generation TiO_2 photocatalysts have been used for air cleaning under indoor daylight or artificial light [182].

However, the activity of photocatalytic wall paints is currently still not satisfactory, and the development of new materials with suitable activity seems to be a challenging task. Although VOCs and bacteria can be degraded by photocatalysts, the removal rate is influenced by numerous parameters: light intensity, pollutant concentration, humidity and so on. Additionally, the generation of relatively stable reaction intermediates (such as the formation of benzaldehyde, benzoic acid and benzyl alcohol during the photocatalytic oxidation of toluene) may lower the removal rate and even stop the reaction through blocking active sites [183].

4.2.2 Thermal catalysis method

Thermal catalysis has been recently studied for use in indoor air purification; however, its application is presently limited to microbe sterilization and HCHO oxidation

because the complete decomposition of other indoor air pollutants by catalytic oxidation requires a much higher reaction temperature than room temperature.

Photocatalytic disinfection requires use of photon energy and a relatively complex device. Therefore, development of environmentally friendly and economic catalytic disinfection methods is needed. For this purpose, many researchers have drawn attention to the study of antibacterial materials working at room temperature [184,185]. Among the various bactericidal metals such as Cu, Zn, Ag and metal oxides such as AgO, CuO, ZnO, MgO, CaO, Ag-loaded catalysts are known to have a wide bactericidal spectrum and relatively high safety [185]. Previous studies by He's group explored the efficiency of silver-loaded bactericidal catalysts including Ag/Al_2O_3, $AgCl/Al_2O_3$, and $Ag\text{-}Ce/AlPO_4$ in the inactivation of SARS coronavirus, *Escherichia coli*, and yeast [186–188]. These microorganisms could be completely inactivated within 30 min on the Ag/Al_2O_3 surface at room temperature. The addition of Ce efficiently enhanced the dispersion of Ag loaded on the catalyst surface, and inhibited the elution of Ag^+.

Up to now, the bactericidal mechanism of non-photocatalysis technology was controversial. The majority of studies suggest that microorganisms in contact with a catalyst could first cause disruption to bacterial membranes and then apoptosis and decomposition. The core mechanism is the reaction with reactive oxygen species (ROS) generated by the activation of oxygen molecules on the catalyst surface [187–189]. Interfacial forces and electrostatic interactions are probably also important factors in this respect. In addition, the toxicity of free metal ions originating from the catalyst materials cannot be ignored. For Ag/Al_2O_3, $AgCl/Al_2O_3$, and $Ag\text{-}Ce/AlPO_4$ catalysts, the catalytically bactericidal effect should be considered as a synergic action of ROS and Ag^+ [186–189]. In short, catalytic sterilization is a potential technology for air disinfection and purification.

The catalytic oxidation of HCHO has also been investigated over many kinds of materials such as the supported noble metal-based catalysts (Pt, Pd, Rh, Au, Ag) [190–192] or transition metal oxide catalysts (Mn,Sn) [193–195]. OMS-2 shows good activity even in the presence or H_2O; however, noble metal catalysts show much higher activity than metal oxide catalysts. The oxidation of HCHO under ambient conditions has been mainly achieved on Pt-, Pd- and Au-supported catalysts. Among them, Pt-based catalysts were found to be the most effective catalysts for HCHO oxidation at ambient temperature [196]. Zhang et al. first reported in 2005 that a Pt/TiO_2 catalyst could effectively catalyze the HCHO oxidation into H_2O and CO_2 at room temperature [192]. Since then, catalysts with Pt supported on $MnO_x\text{-}CeO_2$ [193], Fe_2O_3 [197], Al_2O_3 and MgO [198] were also investigated and all Pt-based catalysts exhibited high efficiency for ambient HCHO oxidation, revealing that the support has little effect on the catalytic activities. The high activity of the Pt/TiO_2 catalyst has been mainly attributed to the high dispersion of Pt on the support surface and the promotion of oxygen mobility [199]. More recently, it was reported the addition of alkali-metal could significantly improve the activity of Pt/TiO_2 for the ambient HCHO destruction because Na doping further promoted Pt dispersion and induced an atomically dispersed $Pt\text{-}O(OH)_x$–alkali species [192].

The formaldehyde oxidation pathway and intermediates over Pt-base catalysts was also proposed based on the results of in situ DRIFTS experiments. Zhang et al. found that surface dioxymethylene (DOM), formate and CO species are the main reaction intermediates during the HCHO oxidation over Pt/TiO_2 catalysts [196,199]. DOM could be quickly oxidized to formate on the catalyst surface and therefore was hardly observed in spectra. The formate species next decomposed into adsorbed CO species and then was oxidized to CO_2 through reaction with surface oxygen. The decomposition of the formate species into adsorbed CO is the rate determining step [196,199]. Subsequent studies also claimed a similar reaction mechanism for HCHO oxidation over Pt/TiO_2 catalysts at room temperature [200]. Zhang et al. also studied the reaction mechanism of HCHO oxidation over Na-promoted Pt/TiO_2 catalysts using in situ DRIFTS [192]. They observed that Na addition opened a new low-temperature reaction pathway by greatly promoting the activation of surface OH groups and then catalyzing a facile reaction between surface OH and formate species to total oxidation products, rather than the decomposition of formate to CO followed by CO oxidation [192].

5 Water purification by catalysis

Recent treatment methodologies involving catalysis have the potential to treat all types of organic and inorganic contaminants, which include oxidative and reductive processes. The oxidative processes, which are all oxygen based, are usually termed Advanced Oxidation Processes (AOPs). Due to sufficient hydroxyl radicals in the processes, most of organic contaminants are converted into carbon dioxide, short-chain organic acids, and inorganic ions, typically less toxic and amenable to biodegradation. The reductive processes are carried out by the catalytic reduction of metal for the detoxification of halogenated compound and inorganic pollutants in water. In this present, the catalytic materials and catalytic degradation process of contaminants will be summarized for water.

5.1 Catalytic oxidation process in water purification

5.1.1 Heterogeneous Fenton catalysis in water purification

Although the homogeneous Fenton reaction is highly

efficient and low cost for wastewater treatment by detoxification [201], destruction of organic pollutants (dyes, aromatic compounds) [202], and biodegradability improvement [203], it suffers from the drawback of a narrow pH range (pH < 3) and Fe sludge disposal and/or regeneration [204]. The main advantage of developing a heterogeneous Fenton catalyst is the fact that it can help to circumvent the problem of iron oxide sludge formation, and as a result it extends the effective pH range [205]. Moreover, its recoverability and reusability [206] further ascertain the benefits of application.

Iron oxides/metal doped iron oxides. Iron oxides, such as magnetite, hematite, goethite and ferrihydrite were used directly as heterogeneous Fenton catalysts for the oxidation of azo dye, quinoline, and monoterpene [207,208]. Different catalytic mechanism of pollutants degradation was also proposed. For example, as shown in Fig. 4, the reaction may experience an iron cycling on the surface of goethite and •OH radical was involved in the pollutants degradation process.

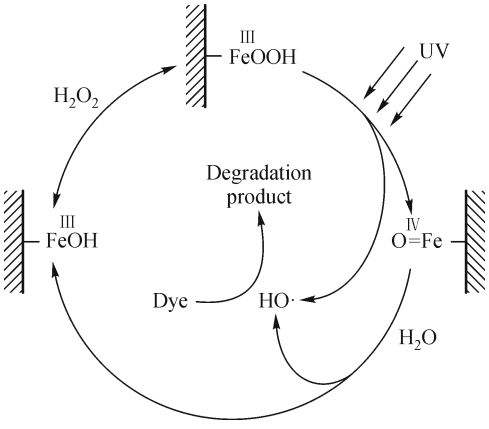

Fig. 4 Schematic diagram of the Fe(III)-initiated Fenton-like chain reaction [209]

Modifications of the iron oxides' structure by doping with other transition-metal cation or by thermal treatment (controlled reduction with H_2) have also been studied in attempt to improve the catalytic performance of those materials [210–212]. It has been proven that the introduction of Mn and Co into Fe_3O_4 resulted in a remarkable increase in the Fenton activity for the oxidation of organic molecules [211,213]. The degradation process takes place via radical species, which can be generated by Fe^{2+}, Co^{2+} and Mn^{2+}. The high activity could be attributed to thermodynamically favorable reduction of Co^{3+} and Mn^{3+} by Fe^{2+} by an electron transfer within the semiconductor oxide. The regeneration of Co^{2+} and Mn^{2+} by this process would be responsible for the remarkable increase on the activity of H_2O_2 decomposition and organic oxidation. Similarly, Cu-doped α-FeOOH, Bi_2O_3 and $LaTiO_3$ perovskite prepared by Hu et al. [214,215] are all followed the same catalytic mechanism. These catalysts exhibited high efficiency for the abatement of dye pollutant and endocrine disruptors.

Metal ion incorporated in different supports. Supported transition-metal ions (Cu^{2+}, Fe^{3+}) are another type promising Fenton catalysts, and the supports can be organic and inorganic materials, such as zeolite, clay, activated carbon, alginate gel beads, Nafion membrane, cationic exchange resin, collagen fiber etc. Metal ions could be anchored onto the surface of support by ion exchange and participated in the Fenton catalytic cycle. For example, Zhao [204] and Hu [216] reported Fe(III)-loaded resin could eliminate dye pollutants and salicylic acid efficiently without leaching out of a significant amount iron ion.

Figure 5 revealed that Fe^{2+} species was generated from the interaction of Fe^{3+} and excited dye molecule via one-electron transfer, leading to the formation of •OH radicals. The resin not only acts as a support for Fe^{2+} and an adsorbent toward the pollutants in solution, but also provides a special microenvironment for active iron centers, enhancing the catalytic decomposition of H_2O_2 even at neutral pH values.

Besides that, Fe^{III} exchanged HY [217] was efficient in the photo-Fenton degradation of phenol at a wide pH range. The enhanced activity was due to the synergistic effect of zeolite by adsorption of pollutant facilitating the rate of degradation. Kiwi et al. [218] have reported the degradation of Orange II by Fe-immobilized Nafion membrane in presence of H_2O_2 under solar simulated visible light irradiation. The Nafion membrane seemed effective over many cycles photo degradation at wide pH range without leaching out of a significant amount iron ion. Fe^{2+} species induced by light in the Nafion was suggested to generate the •OH radicals from H_2O_2 decomposition, leading to the dye degradation.

Metal complex, such as metalporphyrin, metalphthalocyanine, metalbipyridine, salen schiff-base and bioactive hemin could mimic peroxidase and P450 enzymes to catalytically activate oxidants (H_2O_2, O_2 and $KHSO_5$) for

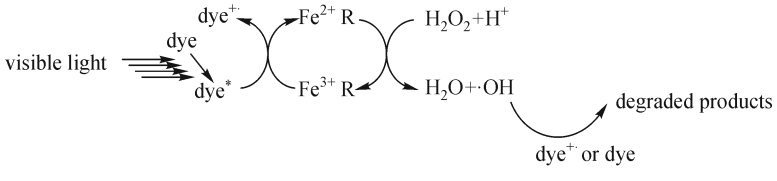

Fig. 5 Proposed Fenton-like mechanism of Fe(III)-resin under visible light irradiation [204]

the degradation of toxic organic pollutants. To immobilize these complexes on different supports such as zeolite, resin and silica gel by molecular impregnation [214], template synthesis [219], or flexible ligand route for the Fenton degradation of organic pollutants has been investigated by many research groups.

Meunier reported for the first time that iron tetrasulfophthalocyanine supported on ion-exchange resin could efficiently degrade 2,4,6-trichlorophenol in the presence of H_2O_2. However, the reaction rate was greatly reduced when water was used as the sole solvent. Moreover, the requirement of an organic cosolvent compound would hinder the application of this treatment method for organic pollutants. To overcome this disadvantage, Zhao [220] has developed a new catalytic system consisting of iron tetrasulfophenylporphyrin ($TPPS_4$) supported on a commercial anionic ion-exchange resin. In comparison with $FeTPPS_4$, the catalyst exhibited much higher efficiency for the photo-Fenton degradation sulforhodamine B and 2,4-dichlorophenol under visible light irradiation.

As show in Fig. 6, upon visible light irradiation, [$HOOFe^{III}$-PR] is converted to [$HOOFe^{III}$-PR]* excited-state transition species, which may undergo intramolecular electron transfer to generate [$Fe^{II}PR$] and $^{\bullet}OOH$ intermediates. Moreover, the O–O band cleavage of [$HOOFe^{III}$-PR]* results in generation of [$PRFe^{Vb}=O$] and $^{\bullet}OH$ radicals. $^{\bullet}OH$ will react immediately with organic pollutants and degrade them effectively.

Besides, in Hu's group, ferrocene was anchored on silica gel by covalent grafting method at ambient conditions. The catalyst also showed high catalytic activity and stability for the degradation of Acid Red B in the presence of H_2O_2 under UVA irradiation [221]. Iron sulfophthalocyanine modified HMS molecular sieve and *β*-cyclodextrin-hemin [222] were further synthesized and highly efficient for the degradation of malachite green, Rhodamine B and 2,4-dichlorophenol at neutral pH in the presence of H_2O_2 and visible light.

Iron hydroxyl/iron oxide-pillared clay. The Fe pillared clay may be one of promising heterogeneous catalyst because of its unique characteristics, abundance and low cost. The hydroxyl-Fe polycation could intercalate clay and be fixed as pillars to form hydroxyl-Fe-pillared clay via cation exchange. Hydroxyl-Fe should be converted to oxide pillars after calcinations at a high temperature through dehydration and dehydroxylation process.

It has been reported that the hydrolysis products of iron ions, such as $Fe(OH)^{2+}$, $Fe(OH)_2^{+}$, $Fe_2(OH)_2^{4+}$ have high photochemistry activity [223,224]. Hydroxyl-Fe pillared clay may also have high photochemistry activity and could be used as a new photo-Fenton catalyst. Hydroxyl-Fe pillared bentonite was successfully developed by Zhu's group [225] and exhibited a high catalytic activity and good long-term stability in multiple runs in the degradation of Orange II. Its catalytic activity for H_2O_2 came from hydroxyl-Fe between sheets rather than Fe^{3+} or Fe^{2+} in tetrahedral or octahedral sheets of bentonite.

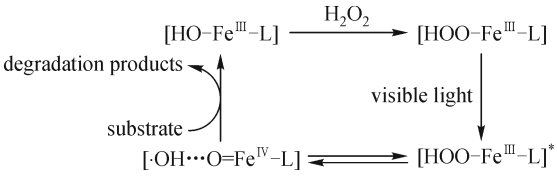

Fig. 6 Proposed photodegradation mechanisms of organic pollutants in the aqueous H_2O_2/FePR system under visible light irradiation [220]

The hydroxyl-Fe-pillared clay would be transformed into α-Fe_2O_3-pillared clay when it was treated with calcinations at 350°C for 24 h. Compared with raw clay, the α-Fe_2O_3-pillared clay possesses large micropore volume and specific surface area as well as more special catalytic activity. For example, Hu [226,227] successfully prepared α-Fe_2O_3-pillared bentonite/laponite as a heterogeneous UV-Fenton catalyst to remove non-biodegradable azo-dye Orange II. The results indicated that the catalyst exhibited a high catalytic activity not only in the photo-Fenton decolorizaion of Orange II but also in the mineralization of Orange II.

5.1.2 Heterogeneous catalytic ozonation in water purification

Heterogeneous catalytic ozonation has received increasing attention in recent years due to its potentially higher effectiveness in the degradation and mineralization of refractory organic pollutants and lower negative effect on water quality. The major advantage of a heterogeneous over a homogeneous catalytic system is the ease of catalytic retrieval from the reaction media. In addition, it has been developed to overcome the limitations of ozonation processes, such as the formation of byproducts and selective reactions of ozone, which are designed to enhance the production of $^{\bullet}OH$.

Several metal oxides such as MnO_2, Al_2O_3, TiO_2, CeO_2, ZnO and FeOOH were studied as possible catalysts for ozonation process. The activity of these catalysts was greatly influenced by temperature and solution pH. MnO_2 is the most widely studied metal oxide as an ozonation catalyst for the removal of atrzine, oxalic acid, pyruvic acid, *N*-methyl-*p*-aminophenol, sulfosalicylic acid and proionic acid. Its activity is known to increase with a decrease of solution pH. Moreover, the structure of MnO_2, resulting from the method of synthesis, is a significant factor determining its activity. For example, the commercial MnO_2 is not active while the pre-formed hydrous MnO_2 (hydrous Mn^{IV}) is slightly lower than MnO_2 formed in situ [228,229]. Al_2O_3 showed high efficiency for the catalytic ozonation of 2-methylisoborneol, 2,4,6-trichloroanisole, chloroethanol, chlorophenol, oxalic acid, acetic and succinic acid [230]. As shown in Fig. 7, the higher

density of surface hydroxyls and stronger surface Brønsted acidity enhanced catalytic activity of Al_2O_3. So that, Al_2O_3 exhibited higher efficiency of catalytic ozonation when compared to ozonation alone.

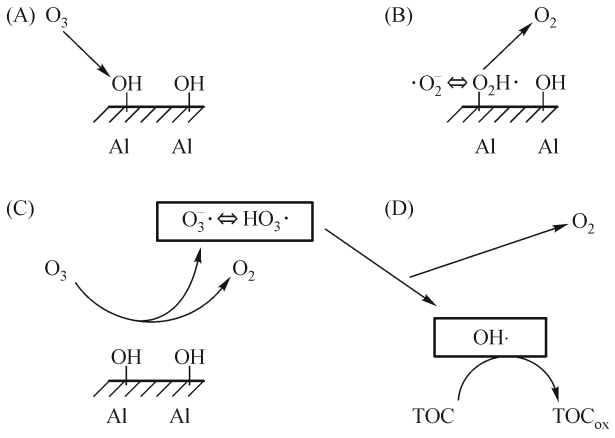

Fig. 7 Suggested reaction mechanism during catalytic ozonation with Al_2O_3 [230]

TiO_2 has been widely used as ozonation catalyst for the degradation of nitrobenzene, 4-chloronitrobenzene, pharmaceuticals (carbamazepine and naproxen) and clofibric acid. Its activity was more dependant on the solution pH and crystal phase structure [201,231]. For example, the O_3/TiO_2 system was found to be efficient for oxalic acid degradation in water at acidic pH and TiO_2 is catalytically active if present in the form of rutile and not anatase.

Zhang et al. reported that among α-FeOOH, β-FeOOH and γ-FeOOH, α-FeOOH exhibited the highest catalytic activity for ozonation of nitrobenzene [232]. The suggested mechanism included ozone decomposition on hydroxyl groups present on the surface of FeOOH leading to hydroxyl radicals generation. Ozone molecular decomposes with the formation of oxygen and Fe–OH($^{\bullet}$O) group. Fe–OH($^{\bullet}$O) subsequently reacts with water leading to the formation of $O_2^{\bullet-}$ and $^{\bullet}$OH radical. Both neutral (Me–OH) and positively charged (Me–OH_2^+) surface groups are responsible for ozone decomposition and $^{\bullet}$OH radicals generation. This catalyst also exhibited good performance for the removal of oxalic acid and p-chlorobenzoic acid.

Co, Mn doped α-Fe_2O_3 and Fe_3O_4 were also found to be effective for the ozonation of 2,4-dichlorophenoxyacetic acid, 2,4-dichlorophenol and 2,4,6-trichlorophenol (herbcides) and phenazone (pharmaceutical) [233,234]. The multivalent oxidation states greatly enhanced the interfacial electron transfer, causing higher catalytic reactivity. Formation of $^{\bullet}$OH radicals resulting from the catalytic decomposition of ozone was found to be the reason for accelerated removal of organic pollutants from the aqueous solution.

Metal oxides such as MnO_2, TiO_2, Fe_2O_3, CoO immobilized on supports (silica gel, clay, PAC, Al_2O_3, ZrO_2 and TiO_2) could also be used as heterogeneous ozonation catalysts for organic compounds removal from water. Their performance was greatly dependent on their method of preparation, thermal history, metal oxides properties and their surface characteristics.

Over 20 ozonation catalysts such as Pt, Pb, Pd, Ag, Co supported on Al_2O_3, SiO_2 and PAC were examined by Lin et al. for the removal of formic acid [235], among which, Pt/Al_2O_3 and Pd/Al_2O_3 exhibited the highest activity. Moreover, solution pH and preparation method significantly influence the activity of the catalyst because they decide about the surface properties. MnO_x supported on mesoporous ZrO_2, Al_2O_3 and CoO_x supported on ZrO_2 have been synthesized by Hu's group and showed high efficiency for the catalytic ozonation of 2,4-dichlorophenoxyacetic acid (herbcides) and phenazone, ibuprofen, diphenhydramine, phenytoin, diclofenac sodium (pharmaceutical) [214,236,237]. The results confirmed that the multivalent oxidation states and high dispersion of MnO_x and CoO_x greatly enhanced the interfacial electron transfer, causing higher catalytic reactivity. The formation of hydroxyl radical resulted in the enhancement of organic pollutants' mineralization.

β-FeOOH supported on mesoporous Al_2O_3 showed high efficiency for the mineralization of ibuprofen and ciprofloxacin aqueous solution with ozone [238]. In comparison with β-FeOOH and MA, surface Lewis acid sites on β-FeOOH/MA were more greatly enhanced and the Lewis acid sites were reactive center for the catalytic ozonation. The stronger Lewis acid sites of β-FeOOH/MA caused the more chemisorbed water enhancing the interaction with ozone, resulting in higher catalytic reactivity.

Cordierite, perovskite, zeolites and ceramic honeycomb are common used as catalysts in ozonation processes for the catalytic ozonation of nitrobenzene, benzophenone, pyruvic acid, gallic acid, phenolic compounds. It was reported by Zhao et al. ceramic honeycomb was an active catalyst of nitrobenzene ozonation [239,240] and $^{\bullet}$OH radicals were involved in the reaction process. Moreover, the surface bound hydroxyl groups are responsible for the formation hydroxyl radicals, therefore, the highest efficiency of this catalyst was observed at pH of solution close to pH_{PZC} of the catalyst. Furthermore, modification of the ceramic honeycomb with Mn, Cu and K could significantly increase the hydroxyl radicals' generation. The reaction mechanism was as following: the uncharged surface bound hydroxyl groups caused ozone decomposition into hydroxyl radicals, resulting in the acceleration of nitrobenzene degradation in bulk solution.

It is well known that activated carbon used together with ozone could provide better removal of color than when the two techniques are used separately. Moreover, activated carbon also showed high efficiency for the removal of phenolic compounds and nitrobenzene in water. Jans and

Hoigne [241] reported that the number of active centers on the surface of activated carbon capable of ozone decomposition is limited, but ozone decomposition and radicals formation are three times faster than in the absence of the catalyst. Hence, ozone decomposition occurs on the surface of activated carbon and hydroxyl radicals formed react with organic molecules in the solution.

Besides, perovskite [242], zeolite and volcanic sand [243] revealed very high catalytic activity in the process of ozonation of gallic acid. Moreover, the efficiency of ozone decomposition was greatly enhanced in the present of ozonation catalyst, leading to greater free radical generation.

5.1.3 Photocatalytic oxidation in water purification

Heterogeneous photocatalysis has been considered as a cost-effective alternative for the destruction of persistent toxic organic compounds [244]. In the process, semiconductor is excited by light energy higher than the band gap, inducing the formation of energy-rich electron-hole pairs, and the charge separation is maintained long enough to react with adsorbed oxygen/H_2O and to produce a series of active oxygen radicals which finally decompose organic compounds as illustrated in previous work [245,246]. TiO_2, ZnO, $SrTiO_3$, CeO_2, WO_3, Fe_2O_3, GaN, Bi_2S_3, CdS and ZnS have been verified to act as photocatalysts in redox/charge-transfer processes due to their electronic structures of a filled valence band and an empty conduction band. Among of them, TiO_2 is the most widely used photocatalytic material because it fulfills all of the above requirements as well as exhibiting adequate conversion values [247]. However, the calculated quantum yield is appreciably low (below 10%) for most degradation in TiO_2 photocatalytic system [248]. As has been known for several decades, an improvement in TiO_2 activity requires the simultaneous control of both morphology and defect structure. Modern photocatalysts are usually high surface area materials, consisting of nanometric particle sizes below 100 nm and typically around 10 nm. It seems obvious, that as the surface area/primary particle size increases/decreases, the number of defective anion and cation surface centers increases. The high photocatalytic reaction rates can be obtained by the limitation of primary particle size at the nanometric range, maximizing specific photoactivity rates per surface area unit if the whole morphology (not only the primary particle size) and defect chemistry of the material are adequately handled. Also, the improvement of TiO_2 optical absorption and photocatalytic performance can be achieved by cation and/or anion doping [244,249]. The photoactivity of anatase-TiO_2 systems was typically enhanced by the addition of noble metals such as Pt, Pd, Ir, and Ag at the oxide surface. These act as electron trapping centers. Also anatase-oxide contact using WO_3, SnO, ZrO_2, or other systems aiming at influencing the electron-hole charge separation process was attempted [244,250]. Solar photocatalysis is expected to be the ideal green technology for water purification. A visible-light-driven photocatalyst has long been anticipated and pursued over recent decades. Recent TiO_2-based catalysts still are not without drawbacks as efficient visible-light-responsive. Therefore, new and/or more efficient visible-light photocatalysts are being sought with a view to meeting the requirements of future environmental and energy technologies driven by solar energy. A large number of alternative photocatalysts exhibiting a great variety of compositions and structures, have been developed [251], having good photocatalytic behavior for pollutant degradation. The new photocatalysts predominantly included perovskite ($A^{2+}B^{4+}O_3$), perovskite-related materials, $A^{3+}B^{5+}O_4$ compounds with scheelite structures and even iron spinels (AB_2O_4). In particular, perovskite-like compounds are stable structures which form solid solutions with a range of metal ions. Hence they are considered promising solids for the chemical substitution of TiO_2 with a view to achieving the appropriate band engineering and consequent band gap lowering required [252]. Furthermore, new nonoxidic structures such as nitrides and sulfides have emerged as promising alternatives for TiO_2 photocatalytic oxidation. Perovskite-structured materials are mainly bismuthate compounds $MBiO_3$ (M = Li, Na, K, Ag), and the ferrite family ($LaFeO_3$, $SrFeO_3$, $BaFeO_3$ and $BiFeO_3$) [253–255]. In general, these catalysts are prepared by hydrothermal synthesis. Different morphologies can be achieved by controlling the parameters of the hydrothermal synthesis. The most interesting result, reported by Ruan et al., refers to the differential photocatalytic behavior observed as a function of the final morphology. So, while microplatelet and nanosheets appear to be photoactive under UV irradiation, nanosheets produce a higher photocatalytic performance under visible irradiation [256]. For Perovskite-Related Structures, Bi_2WO_6 [257] is the simplest and probably the most studied example within this family. Beside this, Bi_2MoO_6 [258], Bi_3O_4Cl (Eg = 2.79 eV) [259], $Na_{0.5}Bi_{1.5}O_2Cl$ (Eg = 3.03 eV) [260] and $PbBiO_2Cl$ (Eg = 2.45 eV) [261], all exhibit visible-light photoactivity. Also related is the fact that other oxyhalides have been proposed which have acceptable photoactivities in the visible range. Oxybromide and oxyiodides such as BiOBr, $PbBiO_2Br$, $BiOI_xBr_{1-x}$ or $BiOI_xCl_{1-x}$ possess good visible light responsive abilities [262]. $BiVO_4$ is scheelite structure, which has been widely reported as exhibiting good photocatalytic properties. Photocatalysis, a heterogeneous type advanced oxidation processes, has been extensively studied for solar energy conversion and purification of water. The generation of hydroxyl radicals by UV or visible photocatalysis for water treatment occurs at the liquid-solid interface, and the subsequent hydroxyl radical reactions are subject to heterogeneous reaction dynamics. At present, the primary drawbacks of photocatalysis still have been the low quantum yields, which

may not be as effective for general water purification processes. However, the growth of heterogeneous photocatalysis will continue to be application-driven, supported by strong process fundamentals. Solar water environmental remediation, which is the mainstay applications, will continue to serve as important platforms for showcasing photocatalytic technologies as well as motivation for establishing relevant fundamental knowledge.

5.2 Catalytic reductive processes in water purification

Reductive catalysis has emerged as a promising water treatment strategy, which offers a more selective transformation of the contaminants to less or nonharmful and more readily biodegradable substances. It is encouraged to be applied to the eliminating of halogenated hydrocarbons [263], nitrate, nitrite perchlorate [264] and *N*-nitrosamines (e.g., NDMA) [265], which being an important class of wastewater-derived micropollutants in water. Several catalysts have been developed for the reductive catalysis in water purification. For example, palladium (Pd)-based catalysis has been extensively studied at the bench-scale, as supported-Pd and Pd-based bimetallic catalysts can activate dihydrogen (H_2) and catalyze reductive transformation of a number of priority drinking water contaminants (Fig. 8).

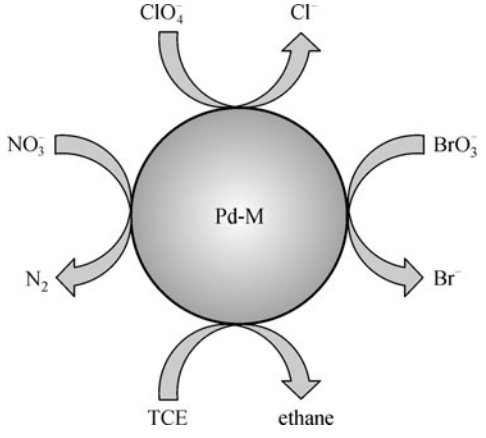

Fig. 8 Schematic showing the transformation of NO_3^-, ClO_4^-, BrO_3^-, and trichloroethylene (TCE) on a Pd-M catalyst particle (M = Cu, In, Re) [266]

Particularly, oxyanions (nitrate, nitrite, bromate, chlorate, perchlorate) [267,268], N-nitrosamines (e.g., *N*-nitrosodimethylamine) [269], and a number of halogenated alkanes (e.g., carbon tetrachloride, 1,2-dichloroethane), alkenes (e.g., trichloroethene, perchloroethene) [270], and aromatics (e.g., chlorinated benzenes, polychlorinated biphenyls) [271]. For example, the nitrogen oxyanions are catalytically reduced to dinitrogen (N_2) and ammonia (NH_3). Beside these, other metals have also been developed for catalytic contaminant reduction, including supported Pt, Ir, Rh, Cu, Zn, Ru (alone or with a promoter metal), and various forms of Ni [272–274]. In general, Pd-based catalysts are more active, stable, and selective for desired end products, and/or less toxic. Here, Pd-based catalysts were focused on published research in the area of catalytic reduction of priority drinking water contaminant, summarizing the characteristics and activity of catalysts, reaction mechanism.

Pd catalysts were doped with other metals to form bimetallic catalysts, having enhanced activity, which has been attributed to the changes in geometric and electronic properties [275]. For example, an alloyed Pd/Au catalyst produced by coprecipitation showed the enhanced activity for the oxidation of CO [276]. A bimetallic core-shell structure, consisting of an Au-core with a Pd-shell increased the activity of Pd nanoparticles for the hydrodechlorination of trichloroethylene by a factor 15 [277]. Moreover, the activity of Au-Pd was increased by a factor 34 [278] by optimization of the particle size (4 nm) and degree of Pd coverage (highest activity with 12.7 wt % Pd) of the Au-nanoparticles. Therefore, in the preparation processes, some metal promoters were added, such as Cu [279], Sn [280], In [279], or Re [281]. Meanwhile, Pd has also been added to ZVI in order to eliminate the need for an external H_2 source (i.e., ZVI corrosion forms H_2), and potentially enhance reaction rates [282]. To increase metal dispersion and facilitate handling and phase separation, Pd and other catalytic metals are often loaded onto support materials. Common supports for contaminant reduction are activated carbon [283], alumina [272,277], and silica [272]. Other less common but effective supports for nitrate and nitrite reduction include TiO_2 [284], ZrO_2 [285], SnO_2 [285], organic resins [286], conducting polymers [287], and carbon nanotubes [288]. An Au support has been shown to be effective for TCE reduction [289], and zeolites are an effective support for reduction of chlorinated aromatics [290].

These supports had indirect effect on activity and selectivity by affecting the density, size, and morphology of catalytic metal clusters on their surfaces [291], and the distribution of reactive sites. Similarly, the preparation methods influence particle morphology and composition [292], and structural changes to the catalyst maybe occur during contaminant reduction [292]. The particle size determined specific surface area to affect catalytic rates and mechanisms [293]. Additionally, supports with high specific surface area or microporosity can have influence on the activity and selectivity of reactions through mass transfer effects [294].

In the catalytic reductive processes, metal catalysts are used to convert hydrogen or other H donor to adsorbed atomic hydrogen (H ads), a powerful reducing agent that reacts with oxidized functional groups. The high functional group selectivity of reductive processes allows for targeted treatment of contaminants within complex mixtures, which is an important factor for the preparation of catalysts.

Proposed reaction pathways for catalytic reduction of several priority contaminants in water have been reported. The reactions predominantly followed three categories: 1) hydrodehalogenation for halogenated organics, 2) hydrodeoxygenation for oxyanions, and 3) N – N hydrogenolysis for N-nitrosamines. Many halogenated organics and some oxyanions can be reduced on Pd alone [295], whereas NO_3^- and ClO_4^- reduction require secondary "promoter" metal.

The important practical challenges are to maximize the activity and selectivity for desired reduction products (N_2 in this case), improve the resistance toward catalyst fouling, and design reactors for full scale applications.

6 Challenges and prospective

Several aspects should be aimed in future research of environmental catalysis for the abatement of major pollutants in air and water. 1) Environment-friendly catalysts have attracted much attention to develop. 2) Significant efforts should be made for the activity and durability of catalysts, and dealing with catalyst fouling for long-term successful treatment. 3) For the selectivity of pollutants transformation to harmfulness should be more concerned by adjusting heterogeneous catalytic processes. 4) Further efforts at materials design or reactor design for pilot- and demonstration-scales. In addition, work is also needed to couple catalytic processes with other treated technologies.

References

1. Busca G, Lietti L, Ramis G, Berti F. Chemical and mechanistic aspects of the selective catalytic reduction of NO_x by ammonia over oxide catalysts: a review. Applied Catalysis B: Environmental, 1998, 18(1–2): 1–36
2. Amiridis M D, Wachs I E, Deo G, Jehng J M, Kim D S. Reactivity of V_2O_5 catalysts for the selective catalytic reduction of NO by NH_3: Influence of vanadia loading, H_2O, and SO_2. Journal of Catalysis, 1996, 161(1): 247–253
3. Liu F D, He H, Zhang C B. Novel iron titanate catalyst for the selective catalytic reduction of NO with NH_3 in the medium temperature range. Chemical Communications, 2008, 17(17): 2043–2045
4. Ma L, Li J H, Ke R, Fu L X. Catalytic Performance, Characterization, and Mechanism Study of $Fe_2(SO_4)_3/TiO_2$ Catalyst for Selective Catalytic Reduction of NO_x by Ammonia. Journal of Physical Chemistry C, 2011, 115(15): 7603–7612
5. Singoredjo L, Korver R, Kapteijn F, Moulijn J. Alumina supported manganese oxides for the low-temperature selective catalytic reduction of nitric-oxide with ammonia. Applied Catalysis B: Environmental, 1992, 1(4): 297–316
6. Shan W, Liu F, He H, Shi X, Zhang C. A superior Ce-W-Ti mixed oxide catalyst for the selective catalytic reduction of NO_x with NH_3. Applied Catalysis B: Environmental, 2012, 115–116: 100–116
7. Liu C X, Chen L, Li J H, Ma L, Arandiyan H, Du Y, Xu J Y, Hao J M. Enhancement of activity and sulfur resistance of CeO_2 supported on TiO_2-SiO_2 for the selective catalytic reduction of NO by NH_3. Environmental Science & Technology, 2012, 46(11): 6182–6189
8. Chen L, Li J H, Ge M F. DRIFT study on cerium-tungsten/titania catalyst for selective catalytic reduction of NO_x with NH_3. Environmental Science & Technology, 2010, 44(24): 9590–9596
9. Pasel J, Kassner P, Montanari B, Gazzano M, Vaccari A, Makowski W, Lojewski T, Dziembaj R, Papp H. Transition metal oxides supported on active carbons as low temperature catalysts for the selective catalytic reduction (SCR) of NO with NH_3. Applied Catalysis B: Environmental, 1998, 18(3–4): 199–213
10. Peng Y, Liu Z, Niu X, Zhou L, Fu C, Zhang H, Li J, Han W. Manganese doped CeO_2-WO_3 catalysts for the selective catalytic reduction of NO_x with NH_3: an experimental and theoretical study. Catalysis Communications, 2012, 19(0): 127–131
11. Topsøe N Y. Mechanism of the selective catalytic reduction of nitric oxide by ammonia elucidated by in situ on-line fourier transform infrared spectroscopy. Science, 1994, 265(5176): 1217–1219
12. Chen L, Li J H, Ge M F. Promotional Effect of Ce-doped V_2O_5-WO_3/TiO_2 with Low Vanadium Loadings for Selective Catalytic Reduction of NO_x by NH_3. Journal of Physical Chemistry C, 2009, 113(50): 21177–21184
13. Li J H, Chang H Z, Ma L, Hao J M, Yang R T. Low-temperature selective catalytic reduction of NO_x with NH_3 over metal oxide and zeolite catalysts-A review. Catalysis Today, 2011, 175(1): 147–156
14. Yang S J, Li J H, Wang C Z, Chen J H, Ma L, Chang H Z, Chen L, Peng Y, Yan N Q. Fe-Ti spinel for the selective catalytic reduction of NO with NH_3: Mechanism and structure-activity relationship. Applied Catalysis B: Environmental, 2012, 117: 73–80
15. Si Z, Weng D, Wu X, Li J, Li G. Structure, acidity and activity of CuO_x/WO_x-ZrO_2 catalyst for selective catalytic reduction of NO by NH_3. Journal of Catalysis, 2010, 271(1): 43–51
16. Li Y, Cheng H, Li D, Qin Y, Xie Y, Wang S. WO_3/CeO_2-ZrO_2, a promising catalyst for selective catalytic reduction (SCR) of NO_x with NH_3 in diesel exhaust. Chemical Communications, 2008, (12): 1470–1472
17. Xu W, Yu Y, Zhang C, He H. Selective catalytic reduction of NO by NH_3 over a Ce/TiO_2 catalyst. Catalysis Communications, 2008, 9(6): 1453–1457
18. Gao X, Jiang Y, Fu Y, Zhong Y, Luo Z, Cen K. Preparation and characterization of CeO_2/TiO_2 catalysts for selective catalytic reduction of NO with NH_3. Catalysis Communications, 2010, 11 (5): 465–469
19. Shan W, Liu F, He H, Shi X, Zhang C. Novel cerium-tungsten mixed oxide catalyst for the selective catalytic reduction of NO_x with NH_3. Chemical Communications, 2011, 47(28): 8046–8048
20. Chen L, Li J H, Ablikim J D, Wang J, Chand H Z, Ma L, Ge M F, Arandiyan H. CeO_2–WO_3 mixed oxides for the selective catalytic reduction of NO_x by NH_3 over a wide temperature range. Catalysis Letters, 2011, 141(12): 1859–1864

21. Dai Y, Li J H, Peng Y, Tang X F. Effects of MnO_2 crystal structure and surface property on the NH_3-SCR reaction at low temperature. Acta Physico-Chimica Sinica, 2012, 28: 1771–1776
22. Kijlstra W S, Biervliet M, Poels E K, Bliek A. Deactivation by SO_2 of MnO_x/Al_2O_3 catalysts used for the selective catalytic reduction of NO with NH_3 at low temperatures. Applied Catalysis B: Environmental, 1998, 16(4): 327–337
23. Tang X, Hao J, Xu W, Li J. Low temperature selective catalytic reduction of NO_x with NH_3 over amorphous MnO_x catalysts prepared by three methods. Catalysis Communications, 2007, 8(3): 329–334
24. Cen W, Liu Y, Wu Z, Wang H, Weng X. A theoretic insight into the catalytic activity promotion of CeO_2 surfaces by Mn doping. Physical Chemistry Chemical Physics, 2012, 14(16): 5769–5777
25. Qi G, Yang R T. Performance and kinetics study for low-temperature SCR of NO with NH_3 over MnO_x-CeO_2 catalyst. Journal of Catalysis, 2003, 217(2): 434–441
26. Chang H Z, Li J H, Chen X Y, Ma L, Yang S J, Schwank J W, Hao J M. Effect of Sn on MnO_x-CeO_2 catalyst for SCR of NO_x by ammonia: Enhancement of activity and remarkable resistance to SO_2. Catalysis Communications, 2012, 27(5): 54–57
27. Qi G S, Yang R T, Chang R. MnO_x-CeO_2 mixed oxides prepared by co-precipitation for selective catalytic reduction of NO with NH_3 at low temperatures. Applied Catalysis B: Environmental, 2004, 51(2): 93–106
28. Casapu M, Krocher O, Elsener M. Screening of doped MnO_x-CeO_2 catalysts for low-templerature NO-SCR. Applied Catalysis B: Environmental, 2009, 88(3–4): 413–419
29. Wang S B, Lu G Q. Effects of acidic treatments on the pore and surface properties of Ni catalyst supported on activated carbon. Carbon, 1998, 36(3): 283–292
30. Kijlstra W S, Brands D S, Poels E K, Bliek A. Mechanism of the selective catalytic reduction of NO by NH_3 over MnO_x/Al_2O_3.1. Adsorption and desorption of the single reaction components. Journal of Catalysis, 1997, 171(1): 208–218
31. Eigenmann F, Maciejewski M, Baiker A. Selective reduction of NO by NH_3 over manganese-cerium mixed oxides: relation between adsorption, redox and catalytic behavior. Applied Catalysis B: Environmental, 2006, 62(3–4): 311–318
32. Yang S J, Wang C Z, Li J H, Yan N Q, Ma L, Chang H Z. Low temperature selective catalytic reduction of NO with NH_3 over Mn–Fe spinel: Performance, mechanism and kinetic study. Applied Catalysis B: Environmental, 2011, 110: 71–80
33. Dunn J P, Stenger H G Jr, Wachs I E. Oxidation of SO_2 over supported metal oxide catalysts. Journal of Catalysis, 1999, 181(2): 233–243
34. Kobayashi M, Hagi M. V_2O_5-WO_3/TiO_2-$SiO_2SO_4^{2-}$ catalysts: Influence of active components and supports on activities in the selective catalytic reduction of NO by NH_3 and in the oxidation of SO_2. Applied Catalysis B: Environmental, 2006, 63(1–2): 104–113
35. Xu W, He H, Yu Y. Deactivation of a Ce/TiO_2 catalyst by SO_2 in the selective catalytic reduction of NO by NH_3. Journal of Physical Chemistry C, 2009, 113(11): 4426–4432
36. Casapu M, Kroecher O, Elsener M. Screening of doped MnO_x-CeO_2 catalysts for low-templerature NO-SCR. Applied Catalysis B: Environmental, 2009, 88(3–4): 413–419
37. Du X, Gao X, Cui L, Fu Y, Luo Z, Cen K. Investigation of the effect of Cu addition on the SO_2-resistance of a Ce–Ti oxide catalyst for selective catalytic reduction of NO with NH_3. Fuel, 2012, 92(1): 49–55
38. Tang X, Hao J, Yi H, Li J. Low-temperature SCR of NO with NH_3 over AC/C supported manganese-based monolithic catalysts. Catalysis Today, 2007, 126(3–4): 406–411
39. Yang S J, Wang C Z, Chen J H, Peng Y, Ma L, Chang H Z, Chen L, Liu C X, Xu J Y, Li J H, Yan N Q. A novel magnetic Fe–Ti–V spinel catalyst for the selective catalytic reduction of NO with NH_3 in a broad temperature range. Catalysis Science & Technology, 2012, 2(5): 915–917
40. Chang H Z, Li J H, Yuan J, Chen L, Dai Y, Arandiyan H, Xu J Y, Hao J M. Ge. Mn-doped CeO_2–WO_3 catalysts for NH_3–SCR of NO_x: Effects of SO_2 and H_2 regeneration. Catalysis Today, 2012,
41. Khodayari R, Odenbrand C U I. Regeneration of commercial SCR catalysts by washing and sulphation: effect of sulphate groups on the activity. Applied Catalysis B: Environmental, 2001, 33(4): 277–291
42. Zheng Y J, Jensen A D, Johnsson J E. Deactivation of V_2O_5-WO_3-TiO_2 SCR catalyst at a biomass-fired combined heat and power plant. Applied Catalysis B: Environmental, 2005, 60(3–4): 253–264
43. Lisi L, Lasorella G, Malloggi S, Russo G. Single and combined deactivating effect of alkali metals and HCl on commercial SCR catalysts. Applied Catalysis B: Environmental, 2004, 50(4): 251–258
44. Nicosia D, Czekaj I, Kroecher O. Chemical deactivation of V_2O_5/WO_3-TiO_2 SCR catalysts by additives and impurities from fuels lubrication oils and urea solution - Part II. Characterization study of the effect of alkali and alkaline earth metals. Applied Catalysis B: Environmental, 2008, 77(3–4): 228–236
45. Klimczak M, Kern P, Heinzelmann T, Lucas M, Claus P. High-throughput study of the effects of inorganic additives and poisons on NH_3-SCR catalysts Part I: V_2O_5-WO_3/TiO_2 catalysts. Applied Catalysis B: Environmental, 2010, 95(1–2): 39–47
46. Lietti L, Forzatti P, Ramis G, Busca G, Bregani F. Potassium doping of vanadia/titania de-NO_x catalysts–surface characterization and reactivity study. Applied Catalysis B: Environmental, 1993, 3(1): 13–35
47. Kamata H, Takahashi K, Odenbrand C U I. The role of K_2O in the selective reduction of NO with NH_3 over a $V_2O_5(WO_3)/TiO_2$ commercial selective catalytic reduction catalyst. Journal of Molecular Catalysis A Chemical, 1999, 139(2–3): 189–198
48. Khodayari R, Odenbrand C U I. Regeneration of commercial TiO_2-V_2O_5-WO_3 SCR catalysts used in bio fuel plants. Applied Catalysis B: Environmental, 2001, 30(1–2): 87–99
49. Tang X F, Li J H, Hao J M. Significant enhancement of catalytic activities of manganese oxide octahedral molecular sieve by marginal amount of doping vanadium. Catalysis Communications, 2010, 11(10): 871–875
50. Chen L, Li J, Ge M. The poisoning effect of alkali metals doping over nano V_2O_5-WO_3/TiO_2 catalysts on selective catalytic reduction of NO_x by NH_3. Chemical Engineering Journal, 2011, 170(2–3): 531–537
51. Calatayud M, Minot C. Effect of alkali doping on a V_2O_5/TiO_2

catalyst from periodic DFT calculations. Journal of Physical Chemistry C, 2007, 111(17): 6411–6417

52. Peng Y, Li J H, Chen L, Chen J H, Han J, Zhang H, Han W. Alkali metal poisoning of a CeO_2-WO_3 catalyst used in the selective catalytic reduction of NO_x with NH_3: an experimental and theoretical study. Environmental Science & Technology, 2012, 46(5): 2864–2869
53. Lee S, Lee J, Keener T C. Mercury oxidation and adsorption characteristics of chemically promoted activated carbon sorbents. Fuel Processing Technology, 2009, 90(10): 1314–1318
54. Lu D Y, Granatstein D L, Rose D J. Study of mercury speciation from simulated coal gasification. Industrial & Engineering Chemistry Research, 2004, 43(17): 5400–5404
55. Presto A A, Granite E J, Karash A, Hargis R A, O'Dowd W J, Pennline H W. A kinetic approach to the catalytic oxidation of mercury in flue gas. Energy & Fuels, 2006, 20(5): 1941–1945
56. Eswaran S, Stenger H G. Understanding mercury conversion in selective catalytic reduction (SCR) catalysts. Energy & Fuels, 2005, 19(6): 2328–2334
57. Lee W, Bae G N. Removal of elemental mercury (Hg^0) by nanosized V_2O_5/TiO_2 catalysts. Environmental Science & Technology, 2009, 43(5): 1522–1527
58. Li Y, Murphy P D, Wu C Y, Powers K W, Bonzongo J C. Development of silica/vanadia/titania catalysts for removal of elemental mercury from coal-combustion flue gas. Environmental Science & Technology, 2008, 42(14): 5304–5309
59. Strege J R, Zygarlicke C J, Folkedahl B C, McCollor D P. SCR deactivation in a full-scale cofired utility boiler. Fuel, 2008, 87(7): 1341–1347
60. Wan Q, Duan L, Li J H, Chen L, He K B, Hao J M. Deactivation performance and mechanism of alkali (earth) metals on V_2O_5-WO_3/TiO_2 catalyst for oxidation of gaseous elemental mercury in simulated coal-fired flue gas. Catalysis Today, 2011, 175(1): 189–195
61. Li H, Wu C Y, Li Y, Zhang J. CeO_2-TiO_2 catalysts for catalytic oxidation of elemental mercury in low-rank coal combustion flue gas. Environmental Science & Technology, 2011, 45(17): 7394–7400
62. Yang S, Guo Y, Yan N, Wu D, He H, Xie J, Qu Z, Jia J. Remarkable effect of the incorporation of titanium on the catalytic activity and SO_2 poisoning resistance of magnetic Mn-Fe spinel for elemental mercury capture. Applied Catalysis B: Environmental, 2011, 101(3–4): 698–708
63. Yang S, Guo Y, Yan N, Wu D, He H, Xie J, Qu Z, Yang C, Jia J. A novel multi-functional magnetic Fe-Ti-V spinel catalyst for elemental mercury capture and callback from flue gas. Chemical Communications, 2010, 46(44): 8377–8379
64. Chen L, Li J, Ge M, Ma L, Chang H. Mechanism of Selective Catalytic Reduction of NO_x with NH_3 over CeO_2-WO_3 Catalysts. Chinese Journal of Catalysis, 2011, 32(5): 836–841
65. Wan Q, Duan L, He K, Li J. Removal of gaseous elemental mercury over a CeO_2-WO_3/TiO_2 nanocomposite in simulated coal-fired flue gas. Chemical Engineering Journal, 2011, 170(2–3): 512–517
66. Qi G S, Yang R T. Low-temperature selective catalytic reduction of NO with NH_3 over iron and manganese oxides supported on titania. Applied Catalysis B: Environmental, 2003, 44(3): 217–225
67. Ji L, Sreekanth P M, Smirniotis P G, Thiel S W, Pinto N G. Manganese oxide/titania materials for removal of NO_x and elemental mercury from flue gas. Energy & Fuels, 2008, 22(4): 2299–2306
68. Li J, Yan N, Qu Z, Qiao S, Yang S, Guo Y, Liu P, Jia J. Catalytic oxidation of elemental mercury over the modified catalyst Mn/alpha-Al_2O_3 at lower temperatures. Environmental Science & Technology, 2010, 44(1): 426–431
69. Niksa S, Fujiwara N. Estimating Hg emissions from coal-fired power stations in China. Fuel, 2009, 88(1): 214–217
70. Presto A A, Granite E J. Survey of catalysts for oxidation of mercury in flue gas. Environmental Science & Technology, 2006, 40(18): 5601–5609
71. Granite E J, Pennline H W, Hargis R A. Novel sorbents for mercury removal from flue gas. Industrial & Engineering Chemistry Research, 2000, 39(4): 1020–1029
72. Laudal D L, Brown T D, Nott B R. Effects of flue gas constituents on mercury speciation. Fuel Processing Technology, 2000, 65–66: 157–165
73. Brandenberger S, Kroecher O, Tissler A, Althoff R. The State of the Art in Selective Catalytic Reduction of NO_x by Ammonia Using Metal-Exchanged Zeolite Catalysts. Catalysis Reviews. Science and Engineering, 2008, 50(4): 492–531
74. Ma L, Li J H, Cheng Y S, Lambert C K, Fu L X. Propene poisoning on three typical Fe-zeolites for SCR of NO_x with NH_3: from mechanism study to coating modified architecture. Environmental Science & Technology, 2012, 46(3): 1747–1754
75. Wilken N, Wijayanti K, Kamasamudram K, Currier N W, Vedaiyan R, Yezerets A, Olsson L. Mechanistic investigation of hydrothermal aging of Cu-Beta for ammonia SCR. Applied Catalysis B: Environmental, 2012, 111: 58–66
76. Peden C H F, Kwak J H, Burton S D, Tonkyn R G, Kim D H, Lee J H, Jen H W, Cavataio G, Cheng Y, Lambert C K. Possible origin of improved high temperature performance of hydrothermally aged Cu/beta zeolite catalysts. Catalysis Today, 2012, 184(1): 245–251
77. Li J H, Zhu R H, Cheng Y S, Lambert C K, Yang R T. Mechanism of propene poisoning on Fe-ZSM-5 for selective catalytic reduction of NO($_x$) with ammonia. Environmental Science & Technology, 2010, 44(5): 1799–1805
78. Schwidder M, Heikens S, De Toni A, Geisler S, Berndt M, Brueckner A, Gruenert W. The role of NO_2 in the selective catalytic reduction of nitrogen oxides over Fe-ZSM-5 catalysts: active sites for the conversion of NO and of NO/NO_2 mixtures. Journal of Catalysis, 2008, 259(1): 96–103
79. Iwasaki M, Yamazaki K, Banno K, Shinjoh H. Characterization of Fe/ZSM-5 $DeNO_x$ catalysts prepared by different methods: Relationships between active Fe sites and NH_3-SCR performance. Journal of Catalysis, 2008, 260(2): 205–216
80. Ma L, Chang H Z, Yang S J, Chen L, Fu L X, Li J H. Relations between iron sites and performance of Fe/HBEA catalysts prepared by two different methods for NH_3-SCR. Chemical Engineering Journal, 2012, 209(15): 652–660
81. Iwasaki M, Yamazaki K, Shinjoh H. NO_x reduction performance of fresh and aged Fe-zeolites prepared by CVD: effects of zeolite structure and Si/Al_2 ratio. Applied Catalysis B: Environmental,

2011, 102(1–2): 302–309
82. Brandenberger S, Kroecher O, Casapu M, Tissler A, Althoff R. Hydrothermal deactivation of Fe-ZSM-5 catalysts for the selective catalytic reduction of NO with NH_3. Applied Catalysis B: Environmental, 2011, 101(3–4): 649–659
83. Kwak J H, Tran D, Burton S D, Szanyi J, Lee J H, Peden C H F. Effects of hydrothermal aging on NH_3-SCR reaction over Cu/zeolites. Journal of Catalysis, 2012, 287: 203–209
84. Ye Q, Wang L, Yang R T. Activity, propene poisoning resistance and hydrothermal stability of copper exchanged chabazite-like zeolite catalysts for SCR of NO with ammonia in comparison to Cu/ZSM-5. Applied Catalysis A, General, 2012, 427: 24–34
85. Schmieg S J, Oh S H, Kim C H, Brown D B, Lee J H, Peden C H F, Kim D H. Thermal durability of Cu-CHA NH_3-SCR catalysts for diesel NO_x reduction. Catalysis Today, 2012, 184(1): 252–261
86. Kwak J H, Tran D, Szanyi J, Peden C H F, Lee J H. The effect of copper loading on the selective catalytic reduction of nitric oxide by ammonia over Cu-SSZ-13. Catalysis Letters, 2012, 142(3): 295–301
87. Ren L, Zhu L, Yang C, Chen Y, Sun Q, Zhang H, Li C, Nawaz F, Meng X, Xiao F S. Designed copper-amine complex as an efficient template for one-pot synthesis of Cu-SSZ-13 zeolite with excellent activity for selective catalytic reduction of NO_x by NH_3. Chemical Communications, 2011, 47(35): 9789–9791
88. Rahkamaa-Tolonen K, Maunula T, Lomma M, Huuhtanen M, Keiski R L. The effect of NO_2 on the activity of fresh and aged zeolite catalysts in the NH_3-SCR reaction. Catalysis Today, 2005, 100(3–4): 217–222
89. Ma L, Li J H, Arandiyan H, Shi W B, Liu C X, Fu L X. Influence of calcination temperature on Fe/HBEA catalyst for the selective catalytic reduction of NO_x with NH_3. Catalysis Today, 2012, 184 (1): 145–152
90. Klukowski D, Balle P, Geiger B, Wagloehner S, Kureti S, Kimmerle B, Baiker A, Grunwaldt J D. On the mechanism of the SCR reaction on Fe/HBEA zeolite. Applied Catalysis B: Environmental, 2009, 93(1–2): 185–193
91. Burch R, Breen J P, Meunier F C. A review of the selective reduction of NO_x, with hydrocarbons under lean-burn conditions with non-zeolitic oxide and platinum group metal catalysts. Applied Catalysis B: Environmental, 2002, 39(4): 283–303
92. He H, Yu Y B. Selective catalytic reduction of NO_x over Ag/Al_2O_3 catalyst: from reaction mechanism to diesel engine test. Catalysis Today, 2005, 100(1–2): 37–47
93. Wang X, Xu Y, Yu S, Wang C. The first study of SCR of NO_x by acetylene in excess oxygen. Catalysis Letters, 2005, 103(1–2): 101–108
94. Wang X, Yu Q, Li G, Liu Z. Rate-determining step of selective catalystic reduction of NO by acetylene over HZSM-5. Catalysis Letters, 2008, 123(3–4): 289–293
95. Hu Y, Griffiths K, Norton P R. Surface science studies of selective catalytic reduction of NO: progress in the last ten years. Surface Science, 2009, 603(10–12): 1740–1750
96. Jing G H, Li J H, Yang D, Hao J M. Promotional mechanism of Tungstation on selective catalytic reduction of NO_x by Methane over $In/WO_3/ZrO_2$. Applied Catalysis B: Environmental, 2009, 91 (1–2): 123–134
97. Li J H, Hao J M, Cui X Y, Fu L X. Influence of preparation methods of In_2O_3/Al_2O_3 catalyst on selective catalytic reduction of NO by propene in the presence of oxygen. Catalysis Letters, 2005, 103(1–2): 75–82
98. Shimizu K, Satsuma A, Hattori T. Catalytic performance of Ag-Al_2O_3 catalyst for the selective catalytic reduction of NO by higher hydrocarbons. Applied Catalysis B: Environmental, 2000, 25(4): 239–247
99. Li J H, Zhu Y Q, Ke R, Hao J M. Improvement of catalytic activity and sulfur-resistance of Ag/TiO_2–Al_2O_3 for NO reduction with propene under lean burn conditions. Applied Catalysis B: Environmental, 2008, 80(3–4): 202–213
100. Pârvulescu V I, Cojocaru B, Pârvulescu V, Richards R, Li Z, Cadigan C, Granger P, Miquel P, Hardacre C. Sol–gel-entrapped nano silver catalysts-correlation between active silver species and catalytic behavior. Journal of Catalysis, 2010, 272(1): 92–100
101. Miyadera T. Alumina-supported silver catalysts for the selective reduction of nitric-oxide with propene and oxygen-containing organic-compounds. Applied Catalysis B: Environmental, 1993, 2 (2–3): 199–205
102. Kim M K, Kim P S, Baik J H, Nam I S, Cho B K, Oh S H. DeNO_x performance of Ag/Al_2O_3 catalyst using simulated diesel fuel-ethanol mixture as reductant. Applied Catalysis B: Environmental, 2011, 105(1–2): 1–14
103. Sultana A, Haneda M, Fujitani T, Hamada H. Influence of Al_2O_3 support on the activity of Ag/Al_2O_3 catalysts for SCR of NO with decane. Catalysis Letters, 2007, 114(1): 96–102
104. Shimizu K, Tsuzuki M, Kato K, Yokota S, Okumura K, Satsuma A. Reductive activation of O_2 with H_2-reduced silver clusters as a key step in the H_2-promoted selective catalytic reduction of NO with C_3H_8 over Ag/Al_2O_3. Journal of Physical Chemistry C, 2007, 111 (2): 950–959
105. Korhonen S T, Beale A M, Newton M A, Weckhuysen B M. New insights into the active surface species of silver alumina catalysts in the selective catalytic reduction of NO. Journal of Physical Chemistry C, 2011, 115(4): 885–896
106. She X, Flytzani-Stephanopoulos M. The role of Ag–O–Al species in silver-alumina catalysts for the selective catalytic reduction of NO_x with methane. Journal of Catalysis, 2006, 237(1): 79–93
107. Sazama P, Capek L, Drobna H, Sobalik Z, Dedecek J, Arve K, Wichterlova B. Enhancement of decane-SCR-NO_x over Ag/alumina by hydrogen. Reaction kinetics and in situ FTIR and UV-vis study. Journal of Catalysis, 2005, 232(2): 302–317
108. Yu Y B, He H, Feng Q C. Novel enolic surface species formed during partial oxidation of CH_3CHO, C_2H_5OH, and C_3H_6 on Ag/Al_2O_3: an in situ DRIFTS study. Journal of Physical Chemistry B, 2003, 107(47): 13090–13092
109. Yu Y B, Gao H W, He H. FTIR, TPD and DFT studies of intermediates on Ag/Al_2O_3 during the selective catalytic reduction of NO by C_2H_5OH. Catalysis Today, 2004, 93–95: 805–809
110. He H, Zhang X L, Wu Q, Zhang C B, Yu Y B. Review of Ag/Al_2O_3-reductant system in the selective catalytic reduction of NO_x. Catalysis Surveys from Asia, 2008, 12(1): 38–55
111. Wu Q, He H, Yu Y B. In situ DRIFTS study of the selective reduction of NO_x with alcohols over Ag/Al_2O_3 catalyst: Role of surface enolic species. Applied Catalysis B: Environmental, 2005,

61(1–2): 107–113
112. Wu Q, Gao H, He H. Study on Effect of SO_2 on the Selective Catalytic Reduction of NO_x with Propene over Ag/Al_2O_3 by in Situ DRIFTS. Chinese Journal of Catalysis, 2006, 27(5): 403–408
113. Yu Y B, Song X P, He H. Remarkable influence of reductant structure on the activity of alumina-supported silver catalyst for the selective catalytic reduction of NO_x. Journal of Catalysis, 2010, 271(2): 343–350
114. Takahashi A, Haneda M, Fujitani T, Hamada H. Selective reduction of NO_2 with acetaldehyde over Co/Al_2O_3 in lean conditions. Journal of Molecular Catalysis A Chemical, 2007, 261 (1): 6–11
115. Yu Q, Wang X, Xing N, Yang H, Zhang S. The role of protons in the NO reduction by acetylene over ZSM-5. Journal of Catalysis, 2007, 245(1): 124–132
116. Taatjes C A, Hansen N, McIlroy A, Miller J A, Senosiain J P, Klippenstein S J, Qi F, Sheng L S, Zhang Y W, Cool T A, Wang J, Westmoreland P R, Law M E, Kasper T, Kohse-Höinghaus K. Enols are common intermediates in hydrocarbon oxidation. Science, 2005, 308(5730): 1887–1889
117. Yan Y, Yu Y, He H, Zhao J. Intimate contact of enolic species with silver sites benefits the SCR of NO_x by ethanol over Ag/Al_2O_3. Journal of Catalysis, 2012, 293: 13–26
118. Epling W S, Campbell L E, Yezerets A, Currier N W, Parks J E II. Overview of the fundamental reactions and degradation mechanisms of NO_x storage/reduction catalysts. Catalysis Reviews. Science and Engineering, 2004, 46(2): 163–245
119. Fridell E, Skoglundh M, Westerberg B, Johansson S, Smedler G. NO_x storage in barium-containing catalysts. Journal of Catalysis, 1999, 183(2): 196–209
120. Li J H, Goh G H, Yang X C, Yang R T. Non-thermal plasma-assisted catalytic NO_x storage over $Pt/Ba/Al_2O_3$ at low temperatures. Applied Catalysis B: Environmental, 2009, 90(3–4): 360–367
121. Nova I, Castoldi L, Lietti L, Tronconi E, Forzatti P, Prinetto F, Ghiotti G. NO_x adsorption study over Pt-Ba/alumina catalysts: FT-IR and pulse experiments. Journal of Catalysis, 2004, 222(2): 377–388
122. Wang X, Yu Y, He H. Effects of temperature and reductant type on the process of NO_x storage reduction over $Pt/Ba/CeO_2$ catalysts. Applied Catalysis B: Environmental, 2011, 104(1–2): 151–160
123. Elizundia U, Lopez-Fonseca R, Landa I, Gutierrez-Ortiz M A, Gonzalez-Velasco J R. FT-IR study of NO_x storage mechanism over $Pt/BaO/Al_2O_3$ catalysts. Effect of the Pt-BaO interaction. Topics in Catalysis, 2007, 42–43(1–4): 37–41
124. Wang X, Yu Y, He H. Effect of Co addition to $Pt/Ba/Al_2O_3$ system for NO_x storage and reduction. Applied Catalysis B: Environmental, 2010, 100(1–2): 19–30
125. Jones A P. Indoor air quality and health. Atmospheric Environment, 1999, 33(28): 4535–4564
126. Khan F I, Ghoshal A K. Removal of volatile organic compounds from polluted air. Journal of Loss Prevention in the Process Industries, 2000, 13(6): 527–545
127. Armor J N. Environmental catalysis. Applied Catalysis B: Environmental, 1992, 1(4): 221–256
128. Liotta L F, Ousmane M, Di Carlo G, Pantaleo G, Deganello G, Marci G, Retailleau L, Giroir-Fendler A. Total oxidation of propene at low temperature over Co_3O_4-CeO_2 mixed oxides: role of surface oxygen vacancies and bulk oxygen mobility in the catalytic activity. Applied Catalysis A, General, 2008, 347(1): 81–88
129. Spivey J J. Complete catalytic-oxidation of volatile organics. Industrial & Engineering Chemistry Research, 1987, 26(11): 2165–2180
130. Liotta L F. Catalytic oxidation of volatile organic compounds on supported noble metals. Applied Catalysis B: Environmental, 2010, 100(3–4): 403–412
131. Delimaris D, Ioannides T. VOC oxidation over MnO_x-CeO_2 catalysts prepared by a combustion method. Applied Catalysis B: Environmental, 2008, 84(1–2): 303–312
132. Garcia T, Solsona B, Cazorla-Amoros D, Linares-Solano A, Taylor S H. Total oxidation of volatile organic compounds by vanadium promoted palladium-titania catalysts: Comparison of aromatic and polyaromatic compounds. Applied Catalysis B: Environmental, 2006, 62(1–2): 66–76
133. Benard S, Giroir-Fendler A, Vernoux P, Guilhaume N, Fiaty K. Comparing monolithic and membrane reactors in catalytic oxidation of propene and toluene in excess of oxygen. Catalysis Today, 2010, 156(3–4): 301–305
134. Uzio D, Peureux J, Giroirfendler A, Torres M, Ramsay J, Dalmon J A. Platinum/gamma-Al_2O_3 catalytic membrane–preparation, morphological and catalytic characterizations. Applied Catalysis A, General, 1993, 96(1): 83–97
135. Huang S, Zhang C, He H. Complete oxidation of o-xylene over Pd/Al_2O_3 catalyst at low temperature. Catalysis Today, 2008, 139(1–2): 15–23
136. Centi G. Supported palladium catalysts in environmental catalytic technologies for gaseous emissions. Journal of Molecular Catalysis A Chemical, 2001, 173(1–2): 287–312
137. Tidahy H L, Siffert S, Lamonier J F, Zhilinskaya E A, Aboukais A, Yuan Z Y, Vantomme A, Su B L, Canet X, De Weireld G, Frere M, N'Guyen T B, Giraudon J M, Leclercq G. New Pd/hierarchical macro-mesoporous ZrO_2, TiO_2 and ZrO_2-TiO_2 catalysts for VOCs total oxidation. Applied Catalysis A, General, 2006, 310: 61–69
138. Gelin P, Primet M. Complete oxidation of methane at low temperature over noble metal based catalysts: a review. Applied Catalysis B: Environmental, 2002, 39(1): 1–37
139. Lyubovsky M, Pfefferle L, Datye A, Bravo J, Nelson T. TEM study of the microstructural modifications of an alumina-supported palladium combustion catalyst. Journal of Catalysis, 1999, 187(2): 275–284
140. Zhu H Q, Qin Z F, Shan W J, Shen W J, Wang J G. Low-temperature oxidation of CO over Pd/CeO_2-TiO_2 catalysts with different pretreatments. Journal of Catalysis, 2005, 233(1): 41–50
141. Burch R, Urbano F J. Investigation of the active state of supported palladium catalysts in the combustion of methane. Applied Catalysis A, General, 1995, 124(1): 121–138
142. Yang S W, Maroto-Valiente A, Benito-Gonzalez M, Rodriguez-Ramos I, Guerrero-Ruiz A. Methane combustion over supported palladium catalysts I. Reactivity and active phase. Applied Catalysis B: Environmental, 2000, 28(3–4): 223–233
143. Li W B, Wang J X, Gong H. Catalytic combustion of VOCs on

non-noble metal catalysts. Catalysis Today, 2009, 148(1–2): 81–87
144. Chen J H, Shi W B, Zhang X Y, Arandiyan H, Li D F, Li J H. Roles of Li^{+} and Zr^{4+} cations in the catalytic performances of $Co_{(1-x)}M_xCr_2O_4$ (M = Li, Zr; x = 0–0.2) for methane combustion. Environmental Science & Technology, 2011, 45(19): 8491–8497
145. Chen J H, Shi W B, Yang S J, Arandiyan H, Li J H. Distinguished roles with various vanadium loadings of $CoCr_{2-x}V_xO_4$ (x = 0–0.20) for methane combustion. Journal of Physical Chemistry C, 2011, 115(35): 17400–17408
146. Li J H, Liang X, Xu S C, Hao J M. Manganese-doped cobalt oxides on methane combustion at low temperature. Applied Catalysis B: Environmental, 2009, 90(1–2): 307–312
147. Li J H, Fu H J, Fu L X, Hao J M. Complete combustion of methane over indium tin oxides catalysts. Environmental Science & Technology, 2006, 40(20): 6455–6459
148. Wang X, Kang Q, Li D. Low-temperature catalytic combustion of chlorobenzene over MnO_x–CeO_2 mixed oxide catalysts. Catalysis Communications, 2008, 9(13): 2158–2162
149. Wang X, Kang Q, Li D. Catalytic combustion of chlorobenzene over MnO_x-CeO_2 mixed oxide catalysts. Applied Catalysis B: Environmental, 2009, 86(3–4): 166–175
150. Wu Y, Zhang Y, Liu M, Ma Z. Complete catalytic oxidation of o-xylene over Mn–Ce oxides prepared using a redox-precipitation method. Catalysis Today, 2010, 153(3–4): 170–175
151. Morales M R, Barbero B P, Cadus L E. MnCu catalyst deposited on metallic monoliths for total oxidation of volatile organic compounds. Catalysis Letters, 2011, 141(11): 1598–1607
152. Chen M, Zheng X M. The effect of K and Al over $NiCo_2O_4$ catalyst on its character and catalytic oxidation of VOCs. Journal of Molecular Catalysis A Chemical, 2004, 221(1–2): 77–80
153. Chen M, Fan L, Qi L, Luo X, Zhou R, Zheng X. The catalytic combustion of VOCs over copper catalysts supported on cerium-modified and zirconium-pillared montmorillonite. Catalysis Communications, 2009, 10(6): 838–841
154. Cuervo M R, Díaz E, de Rivas B, López-Fonseca R, Ordóñez S, Gutiérrez-Ortiz J I. Inverse gas chromatography as a technique for the characterization of the performance of Mn/Zr mixed oxides as combustion catalysts. Journal of Chromatography. A, 2009, 1216 (45): 7873–7881
155. Tian W, Yang H, Fan X, Zhang X. Low-temperature catalytic oxidation of chlorobenzene over MnO_x/TiO_2-CNTs nano-composites prepared by wet synthesis methods. Catalysis Communications, 2010, 11(15): 1185–1188
156. Deng J, Zhang L, Dai H, Xia Y, Jiang H, Zhang H, He H. Ultrasound-Assisted Nanocasting Fabrication of Ordered Mesoporous MnO_2 and Co_3O_4 with High Surface Areas and Polycrystalline Walls. Journal of Physical Chemistry C, 2010, 114(6): 2694–2700
157. Xia Y, Dai H, Zhang L, Deng J, He H, Au C T. Ultrasound-assisted nanocasting fabrication and excellent catalytic performance of three-dimensionally ordered mesoporous chromia for the combustion of formaldehyde, acetone, and methanol. Applied Catalysis B: Environmental, 2010, 100(1–2): 229–237
158. Zimowska M, Michalik-Zym A, Janik R, Machej T, Gurgul J, Socha R P, Podobinski J, Serwicka E M. Catalytic combustion of toluene over mixed Cu-Mn oxides. Catalysis Today, 2007, 119(1–4): 321–326
159. Sinha A K, Suzuki K. Three-dimensional mesoporous chromium oxide: a highly efficient material for the elimination of volatile organic compounds. Angewandte Chemie International Edition, 2004, 44(2): 271–273
160. Jones J, Ross J R H. The development of supported vanadia catalysts for the combined catalytic removal of the oxides of nitrogen and of chlorinated hydrocarbons from flue gases. Catalysis Today, 1997, 35(1–2): 97–105
161. Collins J J, Ness R, Tyl R W, Krivanek N, Esmen N A, Hall T A. A review of adverse pregnancy outcomes and formaldehyde exposure in human and animal studies. Regulatory Toxicology and Pharmacology, 2001, 34(1): 17–34
162. Lim M, Zhou Y, Wang L, Rudolph V, Lu G Q. Development and potential of new generation photocatalytic systems for air pollution abatement: an overview. Asia-Pacific Journal of Chemical Engineering, 2009, 4(4): 387–402
163. Hoffmann M R, Martin S T, Choi W Y, Bahnemann D W. Environmental applications of semiconductor photocatalysis. Chemical Reviews, 1995, 95(1): 69–96
164. Yang D, Liu H, Zheng Z, Yuan Y, Zhao J C, Waclawik E R, Ke X, Zhu H. An efficient photocatalyst structure: TiO_2(B) nanofibers with a shell of anatase nanocrystals. Journal of the American Chemical Society, 2009, 131(49): 17885–17893
165. Yu Y, Yu J C, Yu J G, Kwok Y C, Che Y K, Zhao J C, Ding L, Ge W K, Wong P K. Enhancement of photocatalytic activity of mesoporous TiO_2 by using carbon nanotubes. Applied Catalysis A, General, 2005, 289(2): 186–196
166. Zhang J, Xu Q, Feng Z, Li M, Li C. Importance of the relationship between surface phases and photocatalytic activity of TiO_2. Angewandte Chemie International Edition, 2008, 47(9): 1766–1769
167. Hu Y, Li D, Zheng Y, Chen W, He Y, Shao Y, Fu X, Xiao G. $BiVO_4/TiO_2$ nanocrystalline heterostructure: a wide spectrum responsive photocatalyst towards the highly efficient decomposition of gaseous benzene. Applied Catalysis B: Environmental, 2011, 104(1–2): 30–36
168. Zhang Y, Tang Z R, Fu X, Xu Y J. TiO_2-graphene nanocomposites for gas-phase photocatalytic degradation of volatile aromatic pollutant: is TiO_2-graphene truly different from other TiO_2-carbon composite materials? ACS Nano, 2010, 4(12): 7303–7314
169. Xu Y, Zhuang Y, Fu X. New insight for enhanced photocatalytic activity of TiO_2 by doping carbon nanotubes: a case study on degradation of benzene and methyl orange. Journal of Physical Chemistry C, 2010, 114(6): 2669–2676
170. Wang W, Yu J, Xiang Q, Cheng B. Enhanced photocatalytic activity of hierarchical macro/mesoporous TiO_2-graphene composites for photodegradation of acetone in air. Applied Catalysis B: Environmental, 2012, 119: 109–116
171. Hu X, Hu C, Qu J. Photocatalytic decomposition of acetaldehyde and Escherichia coli using $NiO/SrBi_2O_4$ under visible light irradiation. Applied Catalysis B: Environmental, 2006, 69(1–2): 17–23
172. Kim J H, Seo G, Cho D L, Choi B C, Kim J B, Park H J, Kim M W, Song S J, Kim G J, Kato S. Development of air purification device through application of thin-film photocatalyst. Catalysis Today,

2006, 111(3–4): 271–274
173. Ji P, Takeuchi M, Cuong T, Zhang J, Matsuoka M, Anpo M. Recent advances in visible light-responsive titanium oxide-based photocatalysts. Research on Chemical Intermediates, 2010, 36(4): 327–347
174. Zhang J, Wu Y, Xing M, Leghari S A K, Sajjad S. Development of modified N doped TiO_2 photocatalyst with metals, nonmetals and metal oxides. Energy & Environmental Science, 2010, 3(6): 715–726
175. Rehman S, Ullah R, Butt A M, Gohar N D. Strategies of making TiO_2 and ZnO visible light active. Journal of Hazardous Materials, 2009, 170(2–3): 560–569
176. Yu J, Xiang Q, Zhou M. Preparation, characterization and visible-light-driven photocatalytic activity of Fe-doped titania nanorods and first-principles study for electronic structures. Applied Catalysis B: Environmental, 2009, 90(3–4): 595–602
177. Dong F, Wang H, Wu Z, Qiu J. Marked enhancement of photocatalytic activity and photochemical stability of N-doped TiO_2 nanocrystals by Fe^{3+}/Fe^{2+} surface modification. Journal of Colloid and Interface Science, 2010, 343(1): 200–208
178. Dong F, Wang H, Wu Z. One-step "Green" Synthetic approach for mesoporous C-doped titanium dioxide with efficient visible light photocatalytic activity. Journal of Physical Chemistry C, 2009, 113 (38): 16717–16723
179. Dong F, Guo S, Wang H, Li X, Wu Z. Enhancement of the visible light photocatalytic activity of C-doped TiO_2 nanomaterials prepared by a green synthetic approach. Journal of Physical Chemistry C, 2011, 115(27): 13285–13292
180. Qiu X, Miyauchi M, Sunada K, Minoshima M, Liu M, Lu Y, Li D, Shimodaira Y, Hosogi Y, Kuroda Y, Hashimoto K. Hybrid Cu_xO/TiO_2 nanocomposites as risk-reduction materials in indoor environments. ACS Nano, 2012, 6(2): 1609–1618
181. Zhang L, Fu H, Zhu Y. Efficient TiO_2 photocatalysts from surface hybridization of TiO_2 particles with graphite-like carbon. Advanced Functional Materials, 2008, 18(15): 2180–2189
182. Guo S, Wu Z, Zhao W. TiO_2-based building materials: above and beyond traditional applications. Chinese Science Bulletin, 2009, 54(7): 1137–1142
183. Mendez-Roman R, Cardona-Martinez N. Relationship between the formation of surface species and catalyst deactivation during the gas-phase photocatalytic oxidation of toluene. Catalysis Today, 1998, 40(4): 353–365
184. Lei H, Li D Q, Lin Y J, Evans D G, Xue D. Influence of nano-MgO particle size on bactericidal action against *Bacillus subtilis* var. *niger*. Chinese Science Bulletin, 2005, 50(6): 514–519
185. Neal A L. What can be inferred from bacterium-nanoparticle interactions about the potential consequences of environmental exposure to nanoparticles? Ecotoxicology (London, England), 2008, 17(5): 362–371
186. He H, Dong X P, Yang M, Yang Q X, Duan S M, Yu Y B, Han J, Zhang C B, Chen L, Yang X. Catalytic inactivation of SARS coronavirus, Escherichia coli and yeast on solid surface. Catalysis Communications, 2004, 5(3): 170–172
187. Chang Q, He H, Zhao J, Yang M, Qut J. Bactericidal activity of a Ce-promoted Ag/AlPO4 catalyst using molecular oxygen in water. Environmental Science & Technology, 2008, 42(5): 1699–1704
188. Chen M, Yan L, He H, Chang Q, Yu Y, Qu J. Catalytic sterilization of Escherichia coli K 12 on Ag/Al_2O_3 surface. Journal of Inorganic Biochemistry, 2007, 101(5): 817–823
189. Yan L Z, Chen M X, He H, Qu J H. Bactericidal effect of Al_2O_3-supported Ag catalyst. Chinese Journal of Catalysis, 2005, 26(12): 1122–1126
190. Zhang C B, He H, Tanaka K. Perfect catalytic oxidation of formaldehyde over a Pt/TiO_2 catalyst at room temperature. Catalysis Communications, 2005, 6(3): 211–214
191. Wang R H, Li J H. OMS-2 Catalysts for Formaldehyde Oxidation: Effects of Ce and Pt on Structure and Performance of the Catalysts. Catalysis Letters, 2009, 131(3–4): 500–505
192. Zhang C, Liu F, Zhai Y, Ariga H, Yi N, Liu Y, Asakura K, Flytzani-Stephanopoulos M, He H. Alkali-metal-promoted Pt/TiO_2 opens a more efficient pathway to formaldehyde oxidation at ambient temperatures. Angewandte Chemie International Edition, 2012, 51(38): 9628–9632
193. Li J H, Wang R H, Hao J M. Role of lattice oxygen and lewis acid on ethanol oxidation over OMS-2 catalyst. Journal of Physical Chemistry C, 2010, 144(23): 10544–10550
194. Wang R H, Li J H. Effects of precursor and sulfation on OMS-2 catalyst for oxidation of ethanol and acetaldehyde at low temperatures. Environmental Science & Technology, 2010, 44 (11): 4282–4287
195. Chen T, Dou H Y, Li X L, Tang X F, Li J H, Hao J M. Tunnel structure effect of manganese oxides in complete oxidation of formaldehyde. Microporous and Mesoporous Materials, 2009, 122 (1–3): 170–174
196. Zhang C, He H. A comparative study of TiO_2 supported noble metal catalysts for the oxidation of formaldehyde at room temperature. Catalysis Today, 2007, 126(3–4): 345–350
197. An N, Yu Q, Liu G, Li S, Jia M, Zhang W. Complete oxidation of formaldehyde at ambient temperature over supported Pt/Fe_2O_3 catalysts prepared by colloid-deposition method. Journal of Hazardous Materials, 2011, 186(2–3): 1392–1397
198. Huang H, Leung D Y C. Complete elimination of indoor formaldehyde over supported Pt catalysts with extremely low Pt content at ambient temperature. Journal of Catalysis, 2011, 280(1): 60–67
199. Zhang C B, He H, Tanaka K. Catalytic performance and mechanism of a Pt/TiO_2 catalyst for the oxidation of formaldehyde at room temperature. Applied Catalysis B: Environmental, 2006, 65(1–2): 37–43
200. He Y, Ji H. In-Situ DRIFTS Study on Catalytic Oxidation of Formaldehyde over Pt/TiO_2 under Mild Conditions. Chinese Journal of Catalysis, 2010, 31(2): 171–175
201. Beltrán F J, Rivas F J, Montero-de-Espinosa R. Catalytic ozonation of oxalic acid in an aqueous TiO_2 slurry reactor. Applied Catalysis B: Environmental, 2002, 39(3): 221–231
202. Martins R C, Amaral-Silva N, Quinta-Ferreira R M. Ceria based solid catalysts for Fenton's depuration of phenolic wastewaters, biodegradability enhancement and toxicity removal. Applied Catalysis B: Environmental, 2010, 99(1–2): 135–144
203. Lee B D, Hosomi M. Fenton oxidation of ethanol-washed distillation-concentrated benzo(a)pyrene: reaction product identification and biodegradability. Water Research, 2001, 35(9): 2314–

2319

204. Cheng M, Ma W, Li J, Huang Y, Zhao J, Wen Y, Xu Y. Visible-light-assisted degradation of dye pollutants over Fe(III)-loaded resin in the presence of H_2O_2 at neutral pH values. Environmental Science & Technology, 2004, 38(5): 1569–1575
205. Pignatello J J, Oliveros E, Mackay A. Advanced oxidation processes for organic contaiminant destruction based on the Fenton reaction and related chemistry. Environmental Science & Technology, 2006, 36(1): 1–84
206. Luo M, Bowden D, Brimblecombe P. Catalytic property of Fe-Al pillared clay for Fenton oxidation of phenol by H_2O_2. Applied Catalysis B: Environmental, 2009, 85(3–4): 201–206
207. Menini L, Silva M J, Lelis M F F, Fabris J D, Lago R M, Gusevskaya E V. Novel solvent free liquid-phase oxidation of β-pinene over heterogeneous catalysts based on $Fe_{3-x}M_xO_4$ (M = Co and Mn). Applied Catalysis A, General, 2001, 269(1–2): 117–121
208. Kwan W P, Voelker B M. Decomposition of hydrogen peroxide and organic compounds in the presence of dissolved iron and ferrihydrite. Environmental Science & Technology, 2002, 36(7): 1467–1476
209. He J, Ma W, He J, Zhao J, Yu J C. Photooxidation of azo dye in aqueous dispersions of H_2O_2/α-FeOOH. Applied Catalysis B: Environmental, 2002, 39(3): 211–220
210. Costa R C C, Lelis M F F, Oliveria L C A, Fabris J D, Ardisson J D, Rios R R V A, Silva C N, Lago R M. Remarkable effect of Co and Mn on the activity of $Fe_{3-x}M_xO_4$ promoted oxidation of organic contaminants in aqueous medium with H_2O_2. Catalysis Communications, 2003, 4(10): 525–529
211. Costa R C C, Lelis M F F, Oliveira L C, Fabris J D, Ardisson J D, Rios R R V A, Silva C N, Lago R M. Novel active heterogeneous Fenton system based on $Fe_{3-x}M_xO_4$ (Fe, Co, Mn, Ni): the role of M^{2+} species on the reactivity towards H_2O_2 reactions. Journal of Hazardous Materials, 2006, 129(1–3): 171–178
212. Guimaraes I R, Giroto A, Oliveira L C A, Guerreiro M C, Lima D Q, Fabris J D. Synthesis and thermal treatment of cu-doped goethite: oxidation of quinoline through heterogeneous fenton process. Applied Catalysis B: Environmental, 2009, 91(3–4): 591–586
213. Baldrian P, Merhautová V, Gabriel J, Nerud F, Stopka P, Hruby M, Benes M J. Decolorization of synthetic dyes by hydrogen peroxide with heterogeneous catalysis by mixed iron oxides. Applied Catalysis B: Environmental, 2006, 66(3–4): 258–264
214. Yang L, Hu C, Nie Y, Qu J. Catalytic ozonation of selected pharmaceuticals over mesoporous alumina-supported manganese oxide. Environmental Science & Technology, 2009, 43(7): 2525–2529
215. Zhang L, Nie Y, Hu C, Qu J. Enhanced Fenton degradation of Rhodamine B over nanoscaled Cu-doped $LaTiO_3$ perovskite. Applied Catalysis B: Environmental, 2012, 125: 418–424
216. Feng J, Hu X, Yue P L. Degradation of salicylic acid by photo-assisted Fenton reaction using Fe ions on strongly acidic ion exchange resin as catalyst. Chemical Engineering Journal, 2004, 100(1–3): 159–165
217. Noorjahan M, Durga Kumari V, Subrahmanyam M, Panda L. Immobilized Fe(III)-HY: an efficient and stable photo-Fenton catalyst. Applied Catalysis B: Environmental, 2005, 57(4): 291–298
218. Fernandez J, Bandara J, Lopez A, Buffat P, Kiwi J. Photoassisted Fenton degradation of nonbiodegradable azo dye (Orange II) in Fe-free solutions mediated by cation transfer membranes. Langmuir, 1999, 15(1): 185–192
219. Sorokin A, Séris J L, Meunier B. Efficient oxidative dechlorination and aromatic ring cleavage of chlorinated phenols catalyzed by iron sulfophalocyanine. Science, 1995, 28(26): 1163–1166
220. Huang Y, Li J, Ma W, Cheng M, Zhao J, Yu J C. Efficient H_2O_2 oxidation of organic pollutants catalyzed by supported iron sulfophenylporphyrin under visible light irradiation. Journal of Physical Chemistry B, 2004, 108(22): 7263–7270
221. Nie Y, Hu C, Qu J, Hu X. Efficient photodegradation of Acid Red B by immobilized ferrocene in the presence of UVA and H_2O_2. Journal of Hazardous Materials, 2008, 154(1–3): 146–152
222. Huang Y, Ma W, Li J, Cheng M, Zhao J, Wan L, Yu J C. A novel β-CD-Hemin complex photocatalyst for efficient degradation of organic pollutants at neutral pHs under visible irradiation. Journal of Physical Chemistry B, 2003, 107(35): 9409–9414
223. Lunar L, Sicilia D, Rubio S, Pérez-Bendito D, Nickel U. Degradation of photographic developers by Fenton's reagent: condition optimization and kinetics for metol oxidation. Water Research, 2000, 34(6): 1791–1802
224. Park J W, Lee S E, Rhee I K, Kim J E. Transformation of the fungicide chlorothalonil by Fenton reagent. Journal of Agricultural and Food Chemistry, 2002, 50(26): 7570–7575
225. Chen J, Zhu L. Catalytic degradation of Orange II by UV-Fenton with hydroxyl-Fe-pillared bentonite in water. Chemosphere, 2006, 65(7): 1249–1255
226. Feng J, Hu X, Yue P L. Novel bentonite clay-based Fe-nanocomposite as a heterogeneous catalyst for photo-Fenton discoloration and mineralization of Orange II. Environmental Science & Technology, 2004, 38(1): 269–275
227. Feng J, Hu X, Yue P L, Zhu H Y, Lu G Q. Degradation of azo-dye Orange II by a photoassisted Fenton reaction using a novel composite of iron oxide and silicate nanoparticles as a catalyst. Industrial & Engineering Chemistry Research, 2003, 42(10): 2058–2066
228. Nawrocki J, Kasprzyk-Hordern B. The efficiency and mechanisms of catalytic ozonation. Applied Catalysis B: Environmental, 2010, 99(1–2): 27–42
229. Kasprzyk-Hordern B, Ziółek M, Nawrocki J. Catalytic ozonation and methods of enhancing molecular ozone reactions in water treatment. Applied Catalysis B: Environmental, 2003, 46(4): 639–669
230. Ernst M, Lurot F, Schrotter J C. Catalytic ozonation of refractory organic model compounds in aqueous solution by aluminum oxide. Applied Catalysis B: Environmental, 2004, 47(1): 15–25
231. Yang Y, Ma J, Qin Q, Zhai X. Degradation of nitrobenzene by nano-TiO_2 catalyzed ozonation. Journal of Molecular Catalysis A Chemical, 2007, 267(1–2): 41–48
232. Zhang T, Li C, Ma J, Tian H, Qiang Z. Surface hydroxyl groups of synthetic α-FeOOH in promoting OH generation from aqueous ozone: property and activity relationship. Applied Catalysis B: Environmental, 2008, 82(1–2): 131–137
233. Lv A, Hu C, Nie Y, Qu J. Catalytic ozonation of toxic pollutants

over magnetic cobalt and manganese co-doped γ-Fe_2O_3. Applied Catalysis B: Environmental, 2010, 100(1–2): 62–67
234. Lv A, Hu C, Nie Y, Qu J. Catalytic ozonation of toxic pollutants over magnetic cobalt-doped Fe_3O_4 suspensions. Applied Catalysis B: Environmental, 2012, 117–118: 246–252
235. Lin J, Nakajima T, Jomoto T, Hiraiwa K. Effective catalysts for wet oxidation of formic acid by oxygen and ozone. Ozone Science and Engineering, 2000, 22(3): 241–247
236. Xing S, Hu C, Qu J, He H, Yang M. Characterization and reactivity of MnO_x supported on mesoporous zirconia for herbicide 2,4-D mineralization with ozone. Environmental Science & Technology, 2008, 42(9): 3363–3368
237. Hu C, Xing S, Qu J, He H. Catalytic ozonation of herbicide 2,4-D over cobalt oxide supported on mesoporous zirconia. Journal of Physical Chemistry C, 2008, 112(15): 5978–5983
238. Yang L, Hu C, Nie Y, Qu J. Surface acidity and reactivity of *β*-FeOOH/Al_2O_3 for pharmaceuticals degradation with ozone: in situ ATR-FTIR studies. Applied Catalysis B: Environmental, 2010, 97 (3–4): 340–346
239. Zhao L, Ma J, Sun Z, Zhai X. Mechanism of influence of initial pH on the degradation of nitrobenzene in aqueous solution by ceramic honeycomb catalytic ozonation. Environmental Science & Technology, 2008, 42(11): 4002–4007
240. Zhao L, Sun Z, Ma J. Novel relationship between hydroxyl radical initiation and surface group of ceramic honeycomb supported metals for the catalytic ozonation of nitrobenzene in aqueous solution. Environmental Science & Technology, 2009, 43(11): 4157–4163
241. Jans U, Hoigné J. Activated carbon and carbon black catalyzed transformation of aqueous ozone into OH-radicals. Ozone Science and Engineering, 1998, 20(1): 67–90
242. Rivas F J, Carbajo M, Beltrán F J, Acedo B, Gimeno O. Perovskite catalytic ozonation of pyruvic acid in water: operating conditions influence and kinetics. Applied Catalysis B: Environmental, 2006, 62(1–2): 93–103
243. Valdés H, Farfán V J, Manoli J A, Zaror C A. Catalytic ozone aqueous decomposition promoted by natural zeolite and volcanic sand. Journal of Hazardous Materials, 2009, 165(1–3): 915–922
244. Hoffmann M R, Martin S T, Choi W, Bahnemann D W. Environmental applications of semiconductor photocatalysis. Chemical Reviews, 1995, 95(1): 69–96
245. Maldotti A, Molinari A, Amadelli R. Photocatalysis with organized systems for the oxofunctionalization of hydrocarbons by O_2. Chemical Reviews, 2002, 102(10): 3811–3836
246. Linsebigler A L, Lu G, Yates J T. Photocatalysis on TiO_2 surfaces: principles, mechanisms, and selected results. Chemical Reviews, 1995, 95(3): 735–758
247. Fox M A, Dulay M T. Heterogeneous photocatalysis. Chemical Reviews, 1993, 93(1): 341–357
248. Hincapie M, Maldonado M I, Oller I, Gernjak W, Sanchez-Perez J A, Ballesteros M M, Malato S. Solar photocatalytic degradation and detoxification of EU priority substances. Catalysis Today, 2005, 101(3–4): 203–210
249. Kubacka A, Fernandez-García M, Colon G. Nanostructured Ti–M mixed-metal oxides: toward a visible light-driven photocatalyst. Journal of Catalysis, 2008, 254(2): 272–284
250. Kamat P V. Quantum dot solar cells. Semiconductor nanocrystals as light harvesters. Journal of Physical Chemistry C, 2008, 112 (48): 18737–18753
251. Maeda K, Domen K. New non-oxide photocatalysts designed for overall water splitting under visible light. Journal of Physical Chemistry C, 2007, 111(22): 7851–7861
252. Hur S G, Kim T W, Hwang S J, Choy J H. Influences of A- and B-site cations on the physicochemical properties of perovskite-structured $A(In_{1/3}Nb_{1/3}B_{1/3})O_3$ (A = Sr, Ba; B = Sn, Pb) photocatalysts. Journal of Photochemistry and Photobiology A Chemistry, 2006, 183(1–2): 176–181
253. Yang Y, Sun Y, Jiang Y. Structure and photocatalytic property of perovskite and perovskite-related compounds. Materials Chemistry and Physics, 2006, 96(2–3): 234–239
254. Li S, Jing L, Fu W, Yang L, Xin B, Fu H. Photoinduced charge property of nanosized perovskite-type $LaFeO_3$ and its relationships with photocatalytic activity under visible irradiation. Materials Research Bulletin, 2007, 42(2): 203–212
255. Joshi U A, Jang J S, Borse P H, Lee J S. Microwave synthesis of single-crystalline perovskite $BiFeO_3$ nanocubes for photoelectrode and photocatalytic applications. Applied Physics Letters, 2008, 92 (24): 242106–242109
256. Ruan Q J, Zhang W D. Tunable Morphology of $Bi_2Fe_4O_9$ Crystals for photocatalytic oxidation. Journal of Physical Chemistry C, 2009, 113(10): 4168–4173
257. Fu H, Zhang L, Yao W, Zhu Y. Photocatalytic properties of nanosized Bi_2WO_6 catalysts synthesized via a hydrothermal process. Applied Catalysis B: Environmental, 2006, 66(1–2): 100–110
258. Martínez de la Cruz A, Obregon Alfaro S, Lopez Cuellar E, Ortiz Mendez U. Photocatalytic properties of Bi_2MoO_6 nanoparticles prepared by an amorphous complex precursor. Catalysis Today, 2010, 129(1–2): 194–199
259. Lin X, Huang T, Huang F, Wang W, Shi J. Photocatalytic activity of a Bi-based oxychloride Bi_3O_4Cl. Journal of Physical Chemistry B, 2006, 110(48): 24629–24634
260. Lin X, Shan Z, Li K, Wang W, Yang J, Huang F. Photocatalytic activity of a novel Bi-based oxychloride catalyst $Na_{0.5}Bi_{1.5}O_2Cl$. Solid State Sciences, 2007, 9(10): 944–949
261. Shan Z, Wang W, Lin X, Ding H, Huang F. Photocatalytic degradation of organic dyes on visible-light responsive photocatalyst $PbBiO_2Br$. Journal of Solid State Chemistry, 2008, 181(6): 1361–1366
262. Wang W D, Huang F Q, Lin X P, Yang J H. Visible-light-responsive photocatalysts xBiOBr–(1–x)BiOI. Catalysis Communications, 2008, 9(1): 8–12
263. Mackenzie K, Frenzel H, Kopinke F D. Hydrodehalogenation of halogenated hydrocarbons in water with Pd catalysts: reaction rates and surface competition. Applied Catalysis B: Environmental, 2006, 63(3–4): 161–167
264. Hurley K D, Shapley J R. Efficient heterogeneous catalytic reduction of perchlorate in water. Environmental Science & Technology, 2007, 41(6): 2044–2049
265. Frierdich A J, Shapley J R, Strathmann T J. Rapid reduction of N-nitrosamine disinfection byproducts in water with hydrogen and porous nickel catalysts. Environmental Science & Technology,

2008, 42(1): 262–269
266. Chaplin B P, Reinhard M, Schneider W F, Schüth C, Shapley J R, Strathmann T J, Werth C J. Critical review of Pd-based catalytic treatment of priority contaminants in water. Environmental Science & Technology, 2012, 46(7): 3655–3670
267. Horold S, Vorlop K D, Tacke T, Sell M. Development of catalysts for a selective nitrate and nitrite removal from drinking water. Catalysis Today, 1993, 17(1–2): 21–30
268. Hurley K D, Zhang Y X, Shapley J R. Ligand-enhanced reduction of perchlorate in water with heterogeneous Re-Pd/C catalysts. Journal of the American Chemical Society, 2009, 131(40): 14172–14173
269. Davie M G, Shih K, Pacheco F A, Leckie J O, Reinhard M. Palladium-indium catalyzed reduction of N-nitrosodimethylamine: indium as a promoter metal. Environmental Science & Technology, 2008, 42(8): 3040–3046
270. Schreier C G, Reinhard M. Catalytic hydrodehalogenation of chlorinated ethylenes using palladium and hydrogen for the treatment of contaminated water. Chemosphere, 1995, 31(6): 3475–3487
271. Schuth C, Reinhard M. Hydrodechlorination and hydrogenation of aromatic compounds over palladium on alumina in hydrogen-saturated water. Applied Catalysis B: Environmental, 1998, 18(3–4): 215–221
272. Vorlop K D, Prüsse U. Catalytical removing nitrate from water. Environmental catalysis, 1999, 369: 195–218
273. Mikami I, Sakamoto Y, Yoshinaga Y, Okuhara T. Kinetic and adsorption studies on the hydrogenation of nitrate and nitrite in water using Pd-Cu on active carbon support. Applied Catalysis B: Environmental, 2003, 44(1): 79–86
274. Mikami I, Yoshinaga Y, Okuhara T. Rapid removal of nitrate in water by hydrogenation to ammonia with Zr-modified porous Ni catalysts. Applied Catalysis B: Environmental, 2004, 49(3): 173–179
275. Coq B, Figueras F. Bimetallic palladium catalysts: influence of the co-metal on the catalyst performance. Journal of Molecular Catalysis A Chemical, 2001, 173(1–2): 117–134
276. Venezia A M, Liotta L F, Pantaleo G, La Parola V, Deganello G, Beck A, Koppany Z, Frey K, Horvath D, Guczi L. Activity of SiO_2 supported gold-palladium catalysts in CO oxidation. Applied Catalysis A, General, 2003, 251(2): 359–368
277. Nutt M O, Hughes J B, Michael S W. Designing Pd-on-Au bimetallic nanoparticle catalysts for trichloroethene hydrodechlorination. Environmental Science & Technology, 2005, 39(5): 1346–1353
278. Nutt M O, Heck K N, Alvarez P, Wong M S. Improved Pdon-Au bimetallic nanoparticle catalysts for aqueous-phase trichloroethene hydrodechlorination. Applied Catalysis B: Environmental, 2006, 69(1–2): 115–125
279. Pintar A, Batista J, Levec J, Kajiuchi T. Kinetics of the catalytic liquid-phase hydrogenation of aqueous nitrate solutions. Applied Catalysis B: Environmental, 1996, 11(1): 81–98
280. Prusse U, Vorlop K D. Supported bimetallic palladium catalysts for water-phase nitrate reduction. Journal of Molecular Catalysis A Chemical, 2001, 173(1–2): 313–328
281. Hurley K D, Zhang Y X, Shapley J R. Ligand-enhanced reduction of perchlorate in water with heterogeneous Re-Pd/C catalysts. Journal of the American Chemical Society, 2009, 131(40): 14172–14173
282. He F, Zhao D Y. Hydrodechlorination of trichloroethene using stabilized Fe-Pd nanoparticles: Reaction mechanism and effects of stabilizers, catalysts and reaction conditions. Applied Catalysis B: Environmental, 2008, 84(3–4): 533–540
283. Yoshinaga Y, Akita T, Mikami I, Okuhara T. Hydrogenation of nitrate in water to nitrogen over Pd-Cu supported on active carbon. Journal of Catalysis, 2002, 207(1): 37–45
284. Zhang F X, Miao S, Yang Y L, Zhang X, Chen J X, Guan N J. Size-dependent hydrogenation selectivity of nitrate on Pd-Cu/TiO_2 catalysts. Journal of Physical Chemistry C, 2008, 112(20): 7665–7671
285. Gavagnin R, Biasetto L, Pinna F, Strukul G. Nitrate removal in drinking waters: the effect of tin oxides in the catalytic hydrogenation of nitrate by Pd/SnO_2 catalysts. Applied Catalysis B: Environmental, 2002, 38(2): 91–99
286. Neyertz C, Marchesini F A, Boix A, Miro E, Querini C A. Catalytic reduction of nitrate in water: promoted palladium catalysts supported in resin. Applied Catalysis A, General, 2010, 372(1): 40–47
287. Dodouche I, Barbosa D P, Rangel M D, Epron F. Palladium-tin catalysts on conducting polymers for nitrate removal. Applied Catalysis B: Environmental, 2009, 93(1–2): 50–55
288. Chinthaginjala J K, Bitter J H, Lefferts L. Thin layer of carbon-nano-fibers (CNFS) as catalyst support for fast mass transfer in hydrogenation of nitrite. Applied Catalysis A, General, 2010, 383 (1–2): 24–32
289. Nutt M O, Hughes J B, Michael S W. Designing Pd-on-Au bimetallic nanoparticle catalysts for trichloroethene hydrodechlorination. Environmental Science & Technology, 2005, 39(5): 1346–1353
290. Schuth C, Disser S, Schuth F, Reinhard M. Tailoring catalysts for hydrodechlorinating chlorinated hydrocarbon contaminants in groundwater. Applied Catalysis B: Environmental, 2000, 28(3–4): 147–152
291. Henry C R. Surface studies of supported model catalysts. Surface Science Reports, 1998, 31(7–8): 235–325
292. Xie Y B, Cao H B, Li Y P, Zhang Y, Crittenden J C. Highly selective PdCu/amorphous silica-alumina (ASA) catalysts for groundwater denitration. Environmental Science & Technology, 2011, 45(9): 4066–4072
293. Aramendia M A, Borau V, Garcia I M, Jimenez C, Lafont F, Marinas A, Marinas J M, Urbano F J. Influence of the reaction conditions and catalytic properties on the liquid-phase hydrodechlorination of chlorobenzene over palladium-supported catalysts: activity and deactivation. Journal of Catalysis, 1999, 187(2): 392–399
294. Soares O, Orfao J J M, Pereira M F R. Nitrate reduction catalyzed by Pd-Cu and Pt-Cu supported on different carbon materials. Catalysis Letters, 2010, 139(3–4): 97–104
295. Chen H, Xu Z Y, Wan H Q, Zheng J Z, Yin D Q, Zheng S R. Aqueous bromate reduction by catalytic hydrogenation over Pd/Al_2O_3 catalysts. Applied Catalysis B: Environmental, 2010, 96(3–4): 307–313